

An-Najah National University

Faculty of Graduate Studies

**The Effects of Rashba Spin-orbit Interaction
and Magnetic Field on the Thermo-Magnetic
Properties of an Electron Confined in a
Cylindrical Semiconductor Quantum Dot**

By

Hanaa Sameer Rajab

Supervisor

Prof. Mohammad Elsaid

**This Thesis is Submitted in Partial Fulfillment of The Requirements for
The Degree of Master of Physics, Faculty of Graduate Studies, An-
Najah National University, Nablus -Palestine**

2021

**The Effects of Rashba Spin-orbit Interaction and
Magnetic Field on the Thermo-Magnetic Properties
of an Electron Confined in a Cylindrical
Semiconductor Quantum Dot**

By


Hanaa Sameer Rajab

This Thesis was Defended Successfully on 14/4/2021 and approved by:

Defense Committee Members

Signature

– Prof. Mohammad Elsaid / Supervisor


.....

– Assoc. Prof. Muayad Abu Saa / External Examiner


.....

– Dr. Mahmoud Farout / Internal Examiner


.....

III

Dedication

I will dedicate this work to my parents, for everything they have done for me. They always support me to get the best degrees.

To my dearest husband (Ghaith), who shares me all the moments and support me to overcome difficulties to continue moving forward and don't give up. He also provides me with encouragement, to achieve my ambitions successfully.

To my little daughter (Laila).

To my sisters and brothers.

Acknowledgements

Initially, many great praises and thanks to God who give me the health, and knowledgment to successfully completing this thesis. I would like to exhibit my faithful thanks to my advisor and instructor Prof. Mohammed Elsaid for his guidance, assistance, supervision and advising for all stage of my work. In addition, I would like to thank Mr. Ayham Shaer who helps me to use mathematica program. I will never forget my faculty members of physics department for their help and encouragement. Finally, I will express my especial thanks to my friends for their support and question.

الإقرار

أنا الموقعة أدناه مقدمة الرسالة التي تحمل العنوان :

The Effects of Rashba Spin-orbit Interaction and Magnetic Field on the Thermo-Magnetic Properties of an Electron Confined in a Cylindrical Semiconductor Quantum Dot

أقر بأن ما اشتملت عليه هذه الرسالة إنما هي نتاج جهدي الخاص ، باستثناء ما تمت الإشارة إليه
حيثما ورد ، و أنّ هذه الرسالة ككل ، أو أي جزء لم يُقدّم لنيل أي درجة أو لقب علمي أو بحثي لدى
أي مؤسسة تعليمية أو بحثية أخرى.

Declaration

The work provided in this thesis, unless otherwise referenced, is the researcher's own work and has not been submitted elsewhere for any other degree or qualification.

Student's name:

اسم الطالبة: هناء سمير عبد الفتاح رجب

Signature:

التوقيع : هناء سمير رجب

Date:

التاريخ: 14 /4/ 2021

Table of Contents

No.	Contents	Page
	Dedication	III
	Acknowledgement	IV
	Declaration	V
	Table of Contents	VI
	List of Tables	VIII
	List of Figures	IX
	List of Symbols and Abbreviations	XIII
	Abstract	XV
	Chapter one : Introduction	1
1.1	Nanotechnology and Nanoscale	1
1.2	Quantum Dot and its Structures	4
1.3	Application of Quantum Dot	6
1.4	Rashba Spin Orbit Interaction RSOI	7
1.5	Literature Survey	9
1.6	Research Objectives	11
	Chapter Two: Theory and Method of Calculation	13
2.1	Quantum pseudo dot with Zero Rashba Coupling	13
2.2	Hamiltonian of Cylindrical QD with Rashba Coupling	15
2.2.1	Analytical solution	17
2.3	Magnetization and Susceptibility of QD	18
2.4	Heat Capacity and Entropy	20
	Chapter Three: Results and Discussions	21
3.1	GaAs Cylindrical QD with Zero Rashba Effect.	21
3.1.1	Quantum dot Spectra and Statistical Energy	22
3.1.2	Convergency Test and Statistical Energy	23
3.1.3	Heat Capacity	28
3.1.4	Magnetization and Susceptibility	30
3.2	InAs Cylindrical QD with Rashba Effect	36
3.2.1	Energy Spectrum and Statistical Energy	36
3.2.2	Magnetization and Susceptibility of InAs	40
3.2.3	Heat Capacity	46

VII

3.2.4	Entropy	49
	Chapter Four: Conclusions	54
	References	56
	Appendix	62
	الملخص	ب

VIII

List of Tables

No.	Subject	Page
1.1	Classification of quantum confined structures.	2
3.1	The values of the Ground state energy, with changing angular quantum number m from $(-1 \rightarrow 1)$ and the radial quantum number n is taken from $(0 \rightarrow 1)$ at $\omega_0=5\text{meV}$, $\omega_c=1$ Tesla, $L=5\text{nm}$, and $U_0 = 3\text{meV}$.	22

List of Figures

No	Figure	Page
1.1	Effect of quantum confinement on the density of electronic states.	3
1.2	The effect of quantum confinement on the energy levels in semiconductor quantum dots (QDs).	3
1.3	Type-1 QD and Type2	4
1.4	Schematic representation of the GaAs/AlGaAs cylindrical QD under investigation with the dot height L and the radius R.	5
1.5	Confinement potential for QD.	6
1.6	Absorption and emission spectra of QDs.	7
2.1	Rashba Spin Orbit interaction in Spintronic devices.	9
3.1	The energy spectra of an electron at $\omega_0=5\text{meV}$, $U_0=3\text{meV}$, $L=5\text{nm}$, $[\text{n}]_r (0 \rightarrow 1)$, $n_z (0 \rightarrow 1)$, and $m (-1 \rightarrow 1)$.	23
3.2	Statistical average energy (meV) Vs. #basis calculated at different values of T, at $\omega_0 = 4\text{meV}$, $B = 10\text{Tesla}$, $U_0 = 15\text{meV}$, and $L = 5\text{nm}$.	24
3.3	Statistical average energy against B for different values of T (T= 10 K for solid line, =30 K for dashed line=100K for dotted line). At $L=5\text{nm}$, and $U_0 = 5\text{meV}$.	25
3.4	Statistical average energy against B for different values of ω_0 ($\omega_0 = 2\text{meV}$ for solid line, =8meV for dashed line, = 12meV for dotted line).At T= 10 K, $L=5\text{nm}$, and $U_0 = 5\text{meV}$.	26
3.5	Statistical average energy against B for different values of U_0 ($U_0 = 0\text{meV}$ for solid line, = 5meV for dashed line, = 10meV for dotted line). At T= 10 K, $L=5\text{nm}$, and $\omega_0 = 25\text{meV}$.	27
3.6	Statistical average energy against B for different values of L ($L = 2\text{nm}$ for solid line, = 5nm for dashed line, = 10nm for dotted line).At T= 10 K, $U_0=5\text{meV}$, and $\omega_0 = 25\text{meV}$.	27
3.7	Variation of specific heat with temperature for different values of B ($B = 0\text{T}$ for solid line, = 5T for dashed line, = 10T for dotted line).At $\omega_0=25\text{meV}$, $L=20\text{nm}$, and $U_0=6\text{nm}$.	29

3.8	Variation of specific heat with temperature for different values of U_0 ($U_0 = 0.5, 2, 4 \text{ meV}$ from bottom to top). At $L=20\text{nm}$, $B=5\text{T}$, and $\omega_0 = 25\text{meV}$.	30
3.9	Magnetization (M) of GaAs quantum dot as a function of external magnetic field for three different values of T ($T=10\text{K}$ for solid line, $=50\text{K}$ for dashed line, $=150\text{K}$ for dotted line). At $\omega_0 = 25 \text{ meV}$, $L=5\text{nm}$, and $U_0 = 10\text{meV}$.	31
3.10	Magnetic susceptibility (χ) of GaAs quantum dot as a function of external magnetic field for three different values of T ($T=10\text{K}$ for solid line, $=50\text{K}$ for dashed line). At $\omega_0 = 25 \text{ meV}$, $L=5\text{nm}$ and $U_0 = 10\text{meV}$.	32
3.11	Magnetization (M) of GaAs quantum dot as a function of temperature for two different values of B ($B=5\text{T}$ for solid line, $=10\text{T}$ for dashed line). At $T = 10\text{K}$, $L=5\text{nm}$ and $\omega_0 = 25\text{meV}$.	33
3.12	Magnetic Susceptibility (χ) of GaAs quantum dot as a function of Temperature for two different values of magnetic field ($B=5\text{T}$ for solid line, $=10\text{T}$ for dashed line). At $T = 10\text{K}$, $L=5\text{nm}$ and $\omega_0 = 25\text{meV}$.	34
3.13	Magnetization (M) of GaAs quantum dot as a function of external magnetic field for three different values of ω_0 ($\omega_0=5\text{meV}$ for solid line, $=10\text{meV}$ for dashed line, $=15 \text{ meV}$ for dotted line). At $T = 10\text{K}$, $L=5\text{nm}$ and $U_0 = 10\text{meV}$.	35
3.14	Magnetic susceptibility (χ) of GaAs quantum dot as a function of external magnetic field for three different values of ω_0 ($\omega_0=5\text{meV}$ for solid line, $=10\text{meV}$ for dashed line, $=15\text{meV}$ for dotted line). At $T = 10\text{K}$, $L=5\text{nm}$ and $U_0 = 10\text{meV}$.	35
3.15	The calculated energies of a single electron QD versus the magnetic field at $\rho=10 \text{ nm}$ and $\alpha_R = 0 \text{ meV.nm}$. The solid (dashed) curve for $S=1/2(0)$, respectively.	38
3.16	Confinement energy as a function of magnetic field, for two different values of RSOI parameter α_R ($\alpha_R = 40\text{meV.nm}$ for solid line, $\alpha_R = 0 \text{ meV.nm}$ for dashed line). At $\rho=10\text{nm}$.	39
3.17	The statistical energy against the magnetic field B for three different values of T ($T = 0.1 \text{ K}$, 10 , and 20 K from bottom to top). At $\alpha_R=10 \text{ meV.nm}$, $\rho=10\text{nm}$	40

3.18	Magnetization (M) of InAs quantum dot as a function of external magnetic field for two different values of T (T=5K for solid line = 10K for dashed line) .At $\rho=10\text{nm}, \alpha_R=10\text{meV}\cdot\text{nm}$	41
3.19	Magnetic susceptibility (χ) of InAs as a function of external magnetic field for two different values of T (T=5K for solid line = 10K for dashed line). At $\rho=10\text{nm}, \text{and } \alpha_R=10\text{meV}\cdot\text{nm}$	42
3.20	Magnetization (M) of InAs quantum dot as a function of external magnetic field for two different values of Rashba parameter ($\alpha_R = 0 \text{ meV}\cdot\text{nm}$ for solid line $\alpha_R=40 \text{ meV}\cdot\text{nm}$ for dashed line). At $\rho=10\text{nm}, \text{ and } T=10\text{K}$.	43
3.21	Magnetic susceptibility (χ) of InAs quantum dot as a function of external magnetic field for two different values of Rashba parameter ($\alpha_R = 0 \text{ meV}\cdot\text{nm}$ for solid line, $\alpha_R=40 \text{ meV}\cdot\text{nm}$ for dashed line) .At $\rho=10\text{nm}, \text{ and } T=10\text{K}$.	44
3.22	Magnetization (M) of InAs quantum dot as a function of RSOI parameter for two different values of magnetic field (B = 0.5 T for solid line, B=5T for dashed line) .At $\rho=10\text{nm}, \text{ and } T=10\text{K}$.	45
3.23	Magnetic susceptibility (χ) of InAs quantum dot as a function of RSOI parameter for two different values of magnetic field (B = 0.5 T for solid line, B=5 T for dashed line) .At $\rho=10\text{nm}$ and $T=10\text{K}$.	45
3.24	Variation of specific heat with temperature for different values of RSOI parameter $\alpha_R = (0\text{meV}\cdot\text{nm}$ for solid line, $20\text{meV}\cdot\text{nm}$ for dashed line, and $40\text{meV}\cdot\text{nm}$ for dotted line).At B=5Tesla, and $\rho=10\text{nm}$.	47
3.25	Variation of specific heat with temperature for different values of B (B = 0T for solid line, = 2T for dashed line, = 4T for dotted line).At $\alpha_R=10\text{meV}\cdot\text{nm}, \text{ and } \rho=5\text{nm}$.	48
3.26	Specific heat capacity as a function of RSOI parameter for two different value of B (B=5T for solid line, =10T for dashed line) .At $T=10\text{K}, \text{ and } \rho=10\text{nm}$.	49
3.27	Entropy as a function of temperature at three different values of RSOI parameter ($\alpha_R=0\text{meV}\cdot\text{nm}$ for solid line,	50

	=45meV.nm for dashed line, = 90 meV.nm for dotted line). At B=5T, and $\rho=10\text{nm}$.	
3.28	Variation of entropy of InAs quantum dot with temperature at three different value of B (B=0T for dashed line, =2T for solid line, =3T for dotted line). At $\alpha_R=10\text{ meV.nm}$, and $\rho=5\text{nm}$.	51
3.29	Variation of entropy of InAs quantum dot with temperature at three different value of ρ ($\rho=5\text{nm}$ for dashed line, =10nm for solid line, =15nm for dotted line). At $\alpha_R=10\text{meV.nm}$, and B=1T.	52
3.30	Variation of entropy of InAs quantum dot with RSOI parameter at two different value of B (B= 1T for dashed line, =3T for solid line). At T=30K and $\rho=5\text{nm}$.	53

List of Symbols and Abbreviation

D_f	Number of degrees of freedom
D_c	Number of directions of quantum confinement
QD	Quantum Dot
QW	Quantum Well
QWW	Quantum Well Wire
3D	Three Dimension
2D	Two Dimension
1D	One Dimension
0D	Zero Dimension
InAs	Indium Arsenide
GaAs	Gallium Arsenide
SOI	Spin Orbit Interaction
DOS	Density Of States
M	Magnetization
χ	Susceptibility
\mathbf{k}	Wave vector
H	Hamiltonian
α_R	Rashba parameter
\mathbf{P}	Momentum operator
$\boldsymbol{\sigma}$	Pauli matrices
E_n	Energy spectrum
\hbar	Reduced blank constant
$\langle E \rangle$	Average statistical energy
m_0	Rest mass of electron
m^*	Effective mass of electron
A	Magnetic vector potential
\vec{B}	Magnetic field
U_0	Strength of pseudo potential
e	Electron charge
ω_0	Frequency of confinement potential
ω_c	Cyclotron frequency
Ω	Effective cyclotron frequency
a^*	Effective Bohr radius
\hbar	Reduced blank's constant
R^*	Effective Rydberg energy unit
M	Angular Quantum number
meV	milli electron Volt

XIV

nm	Nano meter
k_B	Boltzmann constant
g^*	Effective Landau factor of the electron
T	Temperature
K	Kelvin degree
Ψ	Wave function
L	Height of the cylinder
c_l	Characteristics length of the harmonic oscillator
$F(a, b, c)$	confluent hyper geometric function
a	effective length scale
i	Imaginary number
$\hat{\nabla}$	Gradient operator
c	Speed of light
n	Radial quantum number
λ	Wavelength of the electron
φ	The azimuth angle
Z	Partition function of the system
C_v	Specific Heat Capacity at constant volume
S	Entropy

**The Effects of Rashba Spin-orbit Interaction and Magnetic Field on
the Thermo-Magnetic Properties of an Electron Confined in a
Cylindrical Semiconductor Quantum Dot**

By

Hanaa Sameer Rajab

Supervisor

Prof. Mohammad Elsaid

Abstract

Based on the effective mass approximation, the magnetic properties of cylindrical GaAs quantum pseudo dot with parabolic confinement and cylindrical InAs quantum dot have been investigated in the presence of magnetic field, Pseudo harmonic potential, and Rashba spin-orbit interaction. The Hamiltonian of an electron confined in a Quantum Dot (QD) has been solved analytically to obtain the Eigen energies. The binding energy of the confined electron has been calculated and displayed as a function of various QD physical parameters, we have shown the dependence of the magnetic and thermal quantities like: magnetization (M), magnetic susceptibility (χ), heat capacity (C_v), and entropy (S) of the confined electron in the QD on: magnetic field, confining frequency (ω_0), potential strength (U_0), and temperature (T). Furthermore, the effect of Rashba spin-orbit interaction term, as a key parameter in the field of spintronic, on the magnetic properties has also been studied.

The results reveal that the external magnetic field strength, temperature and confining frequency in addition to Rashba effect affect significantly the magnetic properties of the QD, changing it from diamagnetic to paramagnetic material in InAs material, while GaAs keeps diamagnetic at

ranges of magnetic field strength. The behavior of the heat capacity and entropy are investigated as a function of external magnetic field and quantum dot parameters. Our results are in very good quantitative agreement with the corresponding ones reported in literature.

Chapter One

Introduction

1.1 Nanotechnology and Nanoscale:

Recently, much attentions are paid to the investigation of physics at low dimensional semiconductor structures. Low dimensional semiconductors or nanostructure semiconductors are those have at least one dimension in a nanoscale. Nanoscale means a range from 0 to 100 Nanometers (nm). A nanometer is one-billionth of a meter or 10^{-9} m. The technique of manipulating, creating and controlling of matter at nanoscale dimension is called Nanotechnology [1].

Two main factors make the properties of nanomaterials significantly differ from bulk one. The increase in relative surface area to volume ratio, and quantum confinement effects. Which can change or enhance properties such as reactivity, optical characteristics of nanomaterial [2].

When the size of a particle is decreased, large number of atoms are exist at the surface compared to those inside, and because the growth and catalytic chemical reactions occur at surfaces, then nanomaterial will be much more reactive than bulk one. When we go into nanoscale region, quantum effects can begin to dominate the behavior of matter, affecting the optical, electrical and magnetic properties of materials.

Classification of nanomaterial depends on the number of dimensions of a material, which are outside the nanoscale (<100 nm) range.

The basic type of quantum-confined structure are shown in Table 1.1

Table 1.1: Classification of quantum confined structures

Structure	Number of dimension outside nanoscale	Quantum confinement
Bulk	3	0
Quantum well	2	1
Quantum well wire	1	2
Quantum Dot	0	3

If the number of degrees of freedom are labeled as D_f and the number of directions of quantum confinement are labeled as D_c , then clearly

$$D_c + D_f = 3 \quad (1.1)$$

For all solid-state systems.

A quantum confined structure will be labeled into three groups in the nanoscale range (1-100 nm) as quantum well (QW), quantum well wire (QWW) and quantum dots (QD) [3].

In the absence of quantum effect, in other words, when the dimensions of the confining structure are not comparable to de Broglie wavelength ($d \gg \lambda$), then the particle behaves like a free particle. In this case, the energy states are continuous. However, the reduction of dimensionality in nanostructures to reach the nanoscale, lead to the quantum effect ($d \sim \lambda$) which results in creation of discrete energy levels [4].

In summary, in each confinement direction the continuous energy band component changes to a discrete component characterized by a quantum number n . When the number of confinement dimension is increased, more discrete energy levels can be found, in other words, restriction on the carrier movement will be found. Density of state(DOS), which is defined as the

number of states per unit energy per unit volume, are affected also with the quantum confinement as shown in Fig. 1.1.

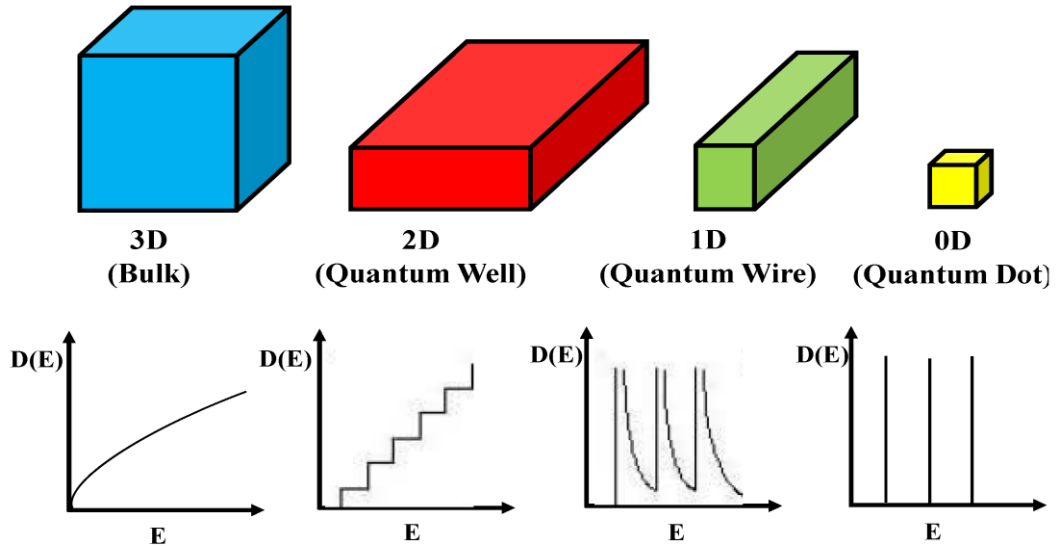


Fig.1.1: Effect of quantum confinement on the density of electronic states [5]

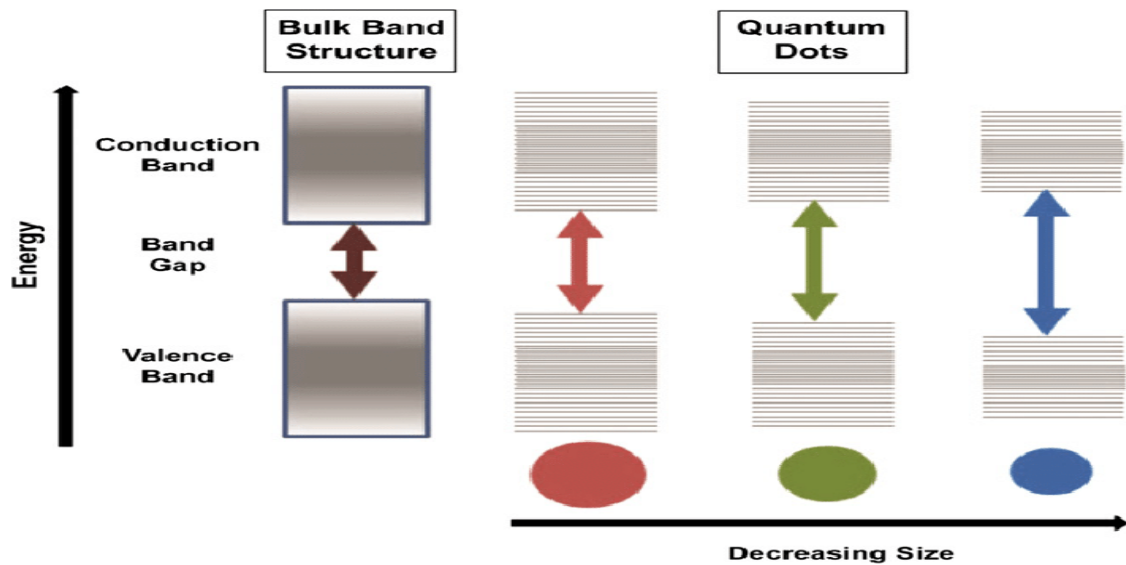


Fig.1.2: The effect of quantum confinement on the energy levels in semiconductor quantum dots (QDs). [6]

1.2 Quantum Dot and its Structures:

Quantum dots (QDs) are nanostructures that confine the carriers (electrons and holes) in three spatial dimensions, thus QD has zero degrees of freedom. Due to this confinement, the energy spectra are fully quantized.

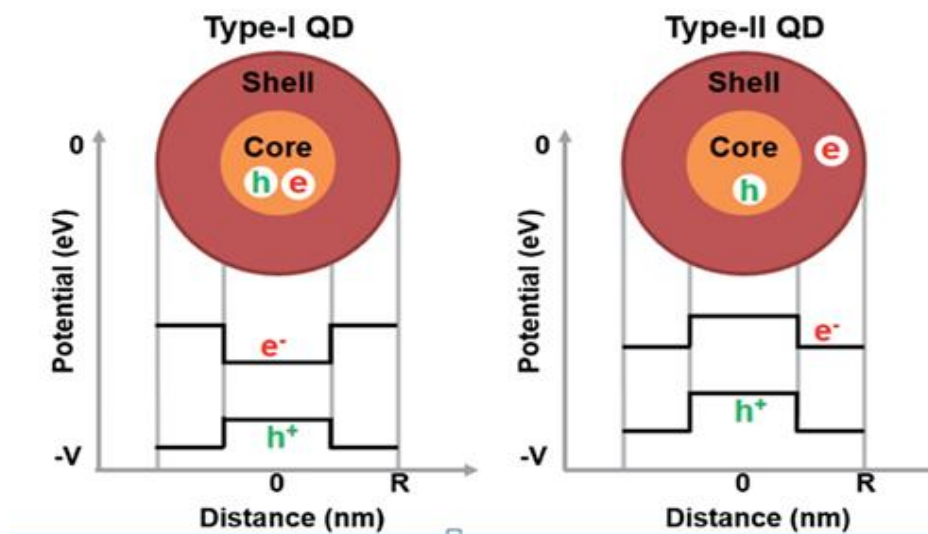


Fig 1.3 Type-1 QD and Type -2. [7]

The main difference between both types is the location of a charge carrier. In structure Type-I both electrons and holes are confined to the core. In type-II, the structure consists of a core where the conduction and valence bands are lower or higher than the shell, which results in one charge carrier in the core and the other confined to the shell.

The properties of a QD's are not only characterized by its size, but also by its shape, composition and structure. In early 1980's, the first QD was successfully made in laboratories. This initiates the investigation of the properties of this heterostructure, and how they are affected and changed

In our research, the GaAs QD is made from Gallium Arsenide (GaAs) surrounded by Aluminum Gallium Arsenide (AlGaAs) semiconductor heterostructure in cylindrical shape, and in the same way the InAs is made , as shown in Fig 1.4.

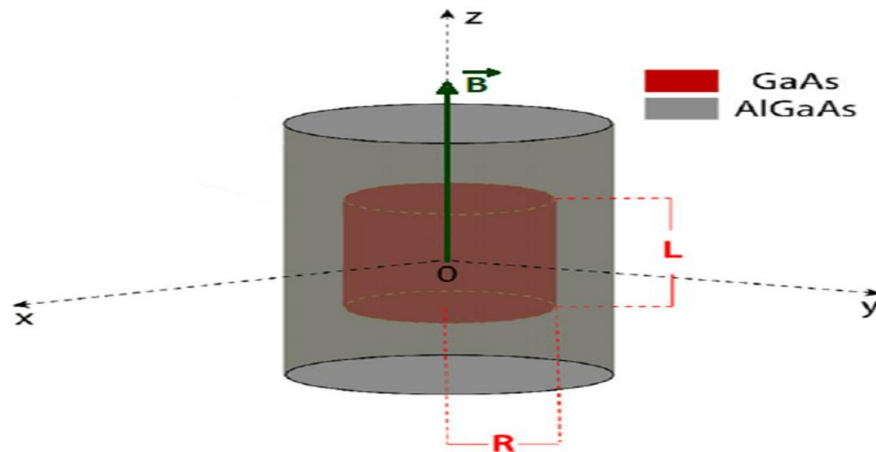


Fig. 1.4: Schematic representation of the GaAs/AlGaAs cylindrical QD in an external magnetic field with the dot height L and the radius R . [8]

To demonstrate our GaAs QD heterostructure, imagine an electron in the XY- plane, at distance r from the origin with confining radial potential $V(r)$ and pseudo –harmonic potential $V(z)$ in the Z –direction, under the influence of external magnetic field in the Z- direction.

Heterostructure consists of layers of two or more semiconductors arranged in a particular way. By applying negative voltage to the metal electrodes on the surface of a heterostructure that contains two dimensional electron gas (2DEG), electrons can be confined to one or zero dimensions and this is how quantum dots are fabricated [9].

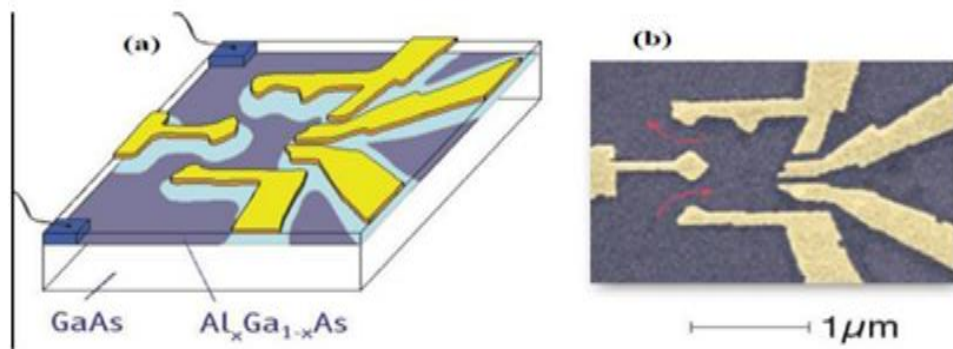


Fig1.5 Confinement potential for QD [10].

1.3 Application of the QDs:

The quantum dots, due to their small nanometer size and the ability of tuning its size and shape during fabrication, will have variety of application in nanotechnology, the main two application are medical and lighting application.

1- Medical Applications and Cancer Treatments:

Nanoparticles can be used as tumor-destroying hyperthermia agents that are injected into the tumor and then be activated to produce heat and destroy cancer cells locally either by magnetic fields, X-Rays or light. When these Quantum dots injected into body the QD's will bind directly to the cancer cell and remove it when they fluoresce.

2- Lighting Applications:

QD's may someday light our homes and streets. When the current is applied directly to the quantum dots layer, it will cause them fluoresce and will be an extremely high efficiency light source. The frequency emitted by quantum

dots can be controlled and manipulate by changing the size of the dots, their shape and material used for their construction. [11]

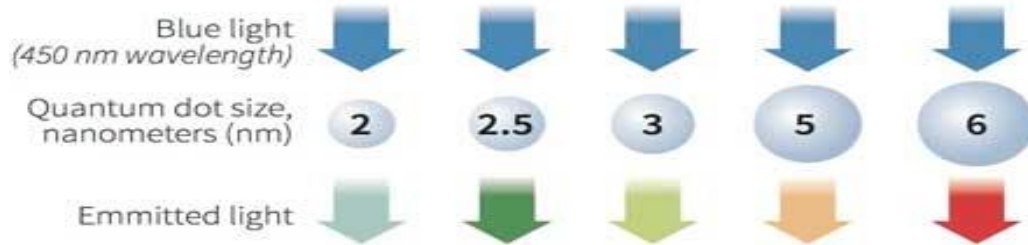


Fig .1.6: The absorption and emission light of a QD's. [12]

1.4 Rashba Spin-Orbit Interaction (RSOI):

The spin-orbit interaction also has an efficient effect in the energy spectrum of electrons confined in QDs. According to the theory of special relativity, electric and magnetic fields are Lorentz transformed when the inertial frame of reference is changed.

Based on relativity concepts, the coupling between spin moment and magnetic field can be analyzed as follow, if an electron is moving in its rest frame, its sees the nucleus as moving charge, these moving charge developed to an internal magnetic field as seen from electron rest frame, and this internal magnetic field interact with the spin moment of the electron.

Spin-orbit coupling phenomena is obviously affecting the energy levels of the electron and its effect is present in physical properties of the system including thermodynamics and magnetic quantities.

The interesting of these phenomena lies in the fact that we can change the asymmetry of the confinement potential by electrostatic one, for example the

ability of tuning the strength of SOI by an external gate voltage. This type of SOI is known as Rashba SOI [13].

The following Hamiltonian describes Rashba SOI:

$$H_R = \frac{\alpha_R}{\hbar} \times [(\vec{p} - q\vec{A}) \times \vec{\sigma}] \cdot \hat{n} \quad (1.2)$$

Where α_R is the Rashba parameter which measures the strength of the SOI, \vec{p} is the momentum operator, and $\vec{\sigma}$ is a vector of Pauli matrices, $q = -e$ is the electron charge, \vec{A} is the vector potential .

The Rashba Hamiltonian, even at zero magnetic field, it removes the spin–degeneracy of the states with the same orbital momentum.

The spin and charge movement, are similar in that they give information about their device but the difference is that the spin direction can be easily manipulated by externally applied magnetic fields [gate-voltage] [14].

The manipulation of the direction of the spin [up down] by an external gate voltage is usually used in technology devise called "Spintronic".

The strength of SOI term can be manipulated experimentally by an external gate voltage or equivalently an applied external electric field through the contact gate with the Heterostructure materials as shown in Figure (1.6).

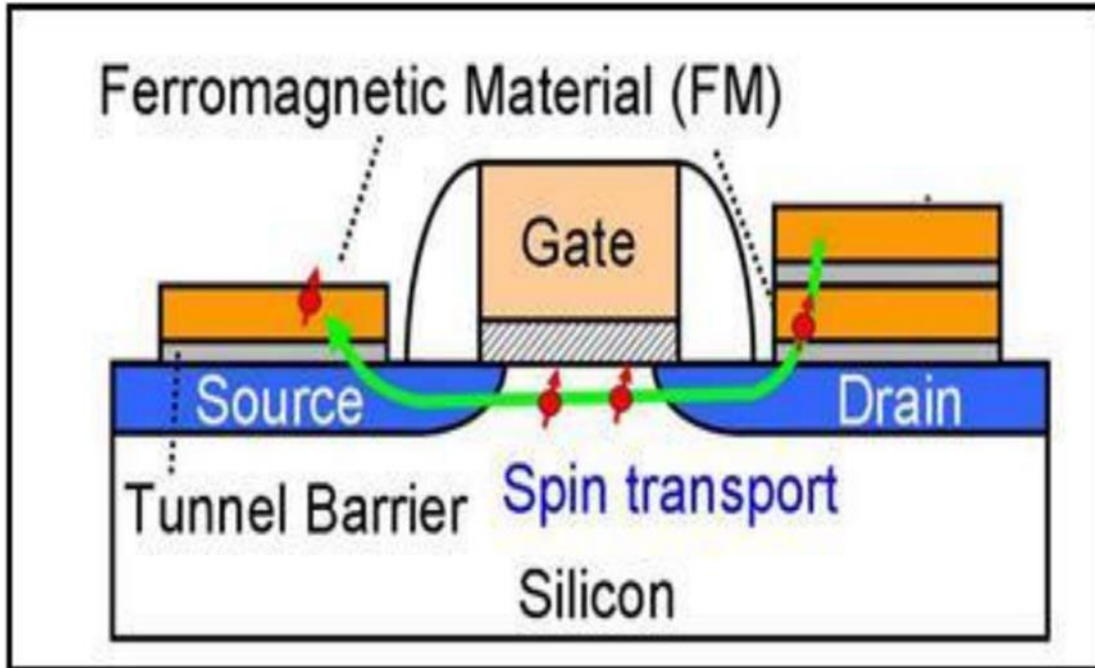


Fig.2.1: Rashba Spin Orbit interaction in Spintronic devices, [15].

1.5 Literature Survey:

Different authors had, recently, studied the thermo- magnetic properties of QD systems in the presence of an external magnetic field.

Ikhdaïr and Hamzavi(2012) calculated the energy levels and the wave functions of an electron confined in a 2D pseudoharmonic quantum dot potential under the influence of temperature and an external magnetic field inside dot and AB field inside a pseudodot by using the Nikiforov-Uvarov method. They computed the exact solutions for energy eigenvalues and wave functions, [16].

Jahromi& Rezaei, (2015), studied the electromagnetically induced transparency in a two-dimensional quantum pseudo-dot system: Effects of geometrical size and external magnetic field, [17].

Khosravi, et.al. (2019), had presented the magnetic Susceptibility of Cylindrical Quantum Dot with Aharonov-Bohm Flux, and Simultaneous Effects of Pressure, Temperature, and Magnetic Field [18].

Yiming Li, et.al.(2001) studied the effect of the sizes and shapes of small semiconductor quantum dots on the electron and hole energy states [19].

Bogachek (2001) studied the temperature scales of magnetization oscillations in an asymmetric quantum dot [20].

Gumber, et.al. (2015) have studied the thermal and magnetic properties of cylindrical quantum dot with asymmetric confinement [21].

Expansion methods to investigate the thermodynamic, electronic and magnetic properties of single and coupled QDs [22].

Shaer, et.al. (2016), studied the Magnetization of GaAs parabolic quantum dot by variation method. [23].

The magnetization (M) and magnetic susceptibility (χ) of a two - electrons parabolic QD in the presence of electron- electron and spin orbit interaction, had been studied by D. Sanjeev Kumar et al.[24].

Elsaid, (2019) studied Magnetic properties of GaAs parabolic quantum dot in the presence of donor impurity under the influence of external tilted electric and magnetic fields. Journal of Taibah University for Science, [25].

Elsaid, (2020) has studied the Rashba spin-orbit interaction effects on thermal and magnetic properties of parabolic GaAs quantum dot in the presence of donor impurity under external electric and magnetic fields, [26].

The magnetization and the magnetic susceptibility of a single electron confined in a two-dimensional (2D) parabolic quantum ring under the effect of external uniform magnetic field and in the presence of an acceptor impurity have been studied by Elsaïd (2020), [27].

The variational and numerical diagonalization techniques have been applied to study the QD Hamiltonian, and investigate the electronic structure, magnetic and thermodynamic properties of a coupled quantum dots, [28-30].

The magnetoabsorption spectra of donors in quantum well wire, has been studied by Elsaïd (1994), [31]

The energy level ordering in two-electron quantum dot spectra. Has been studied by Elsaïd (1998), [32].

In this research, we have studied the effects of the presence of uniform magnetic field and RSOI on the energy spectra and thermodynamic properties of a cylindrical QD with azimuthal symmetry. All the energy matrix elements are obtained in a closed analytical form, then we separate the variable and diagonalize the matrix Hamiltonian and compute the QD energy spectra.

Our results are explicitly displayed in chapter 3.

1.6 Research Objectives:

The main goals of this research project can be summarized as follows:

1-To write the Hamiltonian of a single electron confined in a cylindrical QD subjected to an external magnetic field $\vec{B} = B \hat{Z}$, and radial potential $V(\rho)$ in

x-y plane, and pseudo – harmonic potential $V(z)$ in z-direction, and show how to compute the eigenenergies and eigenfunctions. We have also solved the QD Hamiltonian problem of an electron confined in a semiconductor cylindrical quantum dot subjected to an external magnetic field and SOI, and obtained the eigenenergies and eigenfunction

2- The obtained Eigen energies will be used to study the energy dispersion relation, statistical energy and to investigate the modulation of the properties of the QD by calculating the magnetization (M) and susceptibility (χ) of QD made from GaAs and InAs nanomaterials. In addition, we have used energy spectra to demonstrate the behavior of QD's heat capacity and entropy under the presence of the magnetic field, and the effect of RSOI.

Chapter Two

Theory and Method of Calculation

This chapter contains two parts. In the first part, we present the Hamiltonian of the GaAs cylindrical QD for a single electron confined by a parabolic confinement potential in the presence of the magnetic field and pseudo harmonic potential without Rashba SOI. In the second part, we present the Hamiltonian of the InAs cylindrical quantum dot of an electron confined at the surface of the cylinder in the presence of an external magnetic field, Rashba SOI term and Zeeman term. The main essential step is to reproduce the energy eigenvalues and eigenstates by analytic expression of the QD Hamiltonian. In addition, the mathematical expression for the statistical average energy $\langle E \rangle$, susceptibility (χ), and magnetization (M) are shown.

2.1 Quantum Pseudo Dot with Zero Rashba Coupling:

Within the framework of effective mass approximation, the Hamiltonian of an electron confined by the radial potential $V(\rho) = \frac{1}{2} m^* \omega_0^2 \rho^2$ and pseudo-harmonic potential $V(z) = U_0 \left(\frac{L}{z} - \frac{z}{L} \right)^2$ under the influence of an external magnetic field $\vec{B} = B \hat{z}$ is given by, [33]:

$$H_0 = \frac{1}{2m^*} \left(\vec{P} - \frac{e}{c} \vec{A} \right)^2 + \frac{1}{2} m^* \omega_0^2 \rho^2 + U_0 \left(\frac{L}{z} - \frac{z}{L} \right)^2, \quad (2.1)$$

where m^* is effective mass of the electron that have when interacting with other identical particle in thermal distribution, \vec{P} is the electron momentum operator, \vec{A} is the magnetic vector potential in the Landau gauge $\vec{A} = (A_\rho = 0, A_\phi = B \frac{\rho}{2}, A_z = 0)$, ω_0 is the frequency of confinement potential, U_0 is the

strength of pseudo harmonic potential and L is the height of the cylindrical QD.

The term $U_o \left(\frac{L}{z} - \frac{z}{L} \right)^2$ includes both harmonic quantum dot and anti-dot potential.

The Hamiltonian includes three different terms:

1-The first term is the kinetic energy of the electron, where the quantity $(\vec{p} - \frac{e\vec{A}}{c})$ is known as canonical (total) momentum, \vec{p} is the momentum operator and $e\vec{A}$ is the potential momentum (momentum in field) due to interaction with constant magnetic field acting in the z –direction on the QD.

2-The second term is due to a confinement parabolic potential representing the restriction of the motion of charge carrier, where ω_o is the frequency of the confinement potential.

3- The third term is due to pseudo – harmonic potential in z -direction.

In cylindrical coordinate, the Schrödinger equation can be written as:

$$\begin{aligned} \frac{-\hbar^2}{2m^*} \left[\left(\frac{1}{\rho} \frac{\partial}{\partial \rho} \left(\rho \frac{\partial}{\partial \rho} \right) \right) + \frac{\partial^2}{\partial z^2} + \frac{1}{\rho^2} \frac{\partial^2}{\partial \varphi^2} \right] \psi + \frac{1}{2} \hbar \omega_c L_z \psi + \frac{m^* \omega_c^2 \rho^2}{8} \psi \\ + U_o \left(\frac{L}{z} - \frac{z}{L} \right)^2 \psi + \frac{1}{2} m^* \omega_o^2 \rho^2 \psi = E \psi \end{aligned} \quad (2.2)$$

where $\omega_c = \frac{eB}{m^*c}$ is the Cyclotron frequency.

Separation of variables gives the following eigen functions of the system:

$$\psi = f(\rho, \varphi) \chi(z) \quad (2.3)$$

$$f(\rho, \phi) = \frac{1}{a^{1+|m|}} \sqrt{\frac{(|m|+n)!}{2\pi 2^{|m|} n!}} \frac{1}{m!} \exp\left(\frac{\rho^2}{4a^2}\right) \times \exp(im\phi) \rho^{|m|} F\left(-n, |m|+1, \frac{\rho^2}{2a^2}\right) \quad (2.4)$$

$$\chi(z) = C_{nz} Z^v \exp\left(-\sqrt{\frac{m^* U_0}{2\hbar^2 L^2}} \cdot Z^2\right) \times F\left(-n_z, v + \frac{1}{2}, \sqrt{\frac{m^* U_0}{2\hbar^2 L^2}} \cdot Z^2\right) \quad (2.5)$$

where $\Omega = \sqrt{\omega_c^2 + 4\omega_0^2}$ is the effective frequency, $a = \sqrt{\frac{\hbar}{m^* \Omega}}$ is the effective length scale, $F(a, b, x)$ is the standard confluent hypergeometric function, n is the radial quantum number, m is the magnetic quantum number, C_{nz} is the normalization constant, $v = \frac{1}{2} \sqrt{\frac{8m^* U_0 L^2}{\hbar^2} + 1} + 1$ and n_z is the quantum number.

The total quantum dot Hamiltonian, H , can be reduced to a solvable harmonic oscillator Hamiltonian with analytical energy spectra expression. The eigenenergy spectra is defined, in terms of the quantum numbers (n_r, n_z, m) and other physical parameters, [31]:

$$E = \Omega \hbar \left(n_r + \frac{(1+|m|)}{2} \right) + m \frac{\hbar \omega_c}{2} + \frac{2\hbar}{L} \sqrt{\frac{2U_0}{m^*}} \times \left\{ n_z + \frac{1}{2} + \frac{1}{4} \left[\sqrt{8 m^* U_0 \frac{L^2}{\hbar^2} + 1} - \sqrt{8 m^* U_0 L^2 / \hbar^2} \right] \right\} \quad (2.6)$$

2.2 Hamiltonian of Cylindrical QD with Rashba Coupling:

The Hamiltonian of an electron confined in a cylindrical semiconductor quantum dot subject to an external magnetic field and SOI is given by [34]:

$$H = \frac{(\vec{P} + e\vec{A})^2}{2 m^*} + ((\alpha_R [\vec{\sigma} \times (\vec{P} + e\vec{A})] \cdot \hat{n}))/\hbar + \frac{g \mu_B B \sigma_z}{2} \quad (2.7)$$

where m^* is the effective mass of the electron, g is the effective Lande factor of the electron, $\vec{\sigma}$ is the Pauli matrices, \hat{n} is a unit vector normal to the surface, $\sigma = (\sigma_x, \sigma_y, \sigma_z)$, $\vec{A} = (-B_y/2, B_x/2, 0)$ is the vector potential induced by the magnetic field in the symmetric gauge and α_R is the Rashba parameter which measures the strength of the SOI .

The Hamiltonian consist of three different terms, which are defined as follow:

- 1- The first term is the kinetic energy of the electron, where the quantity $(\mathbf{p} + e\mathbf{A})$ known as canonical (total) momentum, \mathbf{p} is the momentum operator and $e\mathbf{A}$ is the potential momentum (momentum in field) due to the interaction of the electron with constant magnetic field acting in the z –direction on the QD.
- 2- The second term is the Rashba SOI term due to the interaction between orbital angular and spin momenta, where α_R is the Rashba parameter which measures the strength of the SOI and can be varied with the gate voltage, and \hbar is the Plank constant.
- 3- The last term is Zeeman coupling due to an applied external magnetic field along the z –direction $B = (0, 0, B)$, where g is the effective Landau factor of the electron, μ_B is the Bohr magnetron and σ is Pauli spin matrix vector.

2.2.1 Analytical Solution:

The QD Hamiltonian, using the matrix notation, can be written as,[34] .

$$H = \begin{bmatrix} H_{11} & H_{12} \\ H_{21} & H_{22} \end{bmatrix} \text{ With}$$

$$H_{ii} = -\frac{\hbar^2}{2m^*} \left(\frac{\partial^2}{\rho^2 \partial \varphi^2} + \frac{\partial^2}{\partial z^2} \right) + \frac{\hbar \omega_c}{2i} \frac{\partial}{\partial \varphi} + \frac{1}{8} m^* \omega_c^2 \rho^2 \pm \frac{\alpha}{i\rho} \frac{\partial}{\partial \varphi} \pm e \frac{B\alpha\rho}{2\hbar} \pm \frac{1}{2} g\mu_B B \sigma_z. \quad (2.8)$$

The symbol + is for H_{11} and $-$ is for H_{22} , $H_{12} = \alpha e^{-i\varphi} \frac{\partial}{\partial z}$; $H_{21} = \alpha e^{i\varphi} \frac{\partial}{\partial z}$ (2.9)

Where $\omega_c = \frac{eB}{m^*c}$ is the cyclotron frequency. According to the Eqs. (2.8) and (2.9), we find that due to the cylindrical symmetry, the wave functions can be analyzed into a plane wave which is the eigenfunction of the momentum operator and a spinor representing the eigenfunction of the total momentum operator.

$$\begin{pmatrix} \varphi_1^\uparrow(\varphi, z) \\ \varphi_2^\downarrow(\varphi, z) \end{pmatrix} = e^{ik_z z} \begin{pmatrix} e^{im\varphi} f_1 \\ e^{i(m+1)\varphi} f_2 \end{pmatrix} \quad (2.10)$$

where $m=0, \pm 1, \pm 2, \dots$ is the quantum number related to the projection of the angular momentum on the z-direction .Substituting Eq 2.10 into Schrodinger equation yields the following system algebraic equations:

$$\begin{pmatrix} A_{11} & A_{12} \\ A_{21} & A_{22} \end{pmatrix} \begin{pmatrix} f_1 \\ f_2 \end{pmatrix} = 0 \quad (2.11)$$

The adopted notations in Eq. (2.11) are as

$$A_{11} = -k_z^2 \rho^2 - \beta_1 + \lambda_1 + \frac{2m^*}{\hbar^2} \rho^2 \varepsilon \quad (2.12)$$

$$A_{22} = -k_z^2 \rho^2 - \beta_2 + \lambda_2 + \frac{2m^*}{\hbar^2} \rho^2 \varepsilon \quad (2.13)$$

$$A_{12} = -i \frac{2m^*}{\hbar^2} \rho^2 k_z \alpha \quad (2.14)$$

$$A_{21} = i \frac{2m^*}{\hbar^2} \rho^2 k_z \alpha \quad (2.15)$$

Where ε is energy eigenvalues. The parameters β_1 , β_2 and λ_1 , λ_2 are defined as:

$$\beta_1 = m \left[\frac{2m^* \alpha \rho}{\hbar^2} + m + \frac{eB}{\hbar} \rho^2 \right] \quad (2.16)$$

$$\lambda_1 = \frac{-6m^* \rho^2}{\hbar^2} - \frac{m^* g \mu_B B \rho^2}{\hbar^2} - \frac{e \alpha m^* \rho^3 B}{\hbar^3} - \frac{1}{4} \left(\frac{eB \rho^2}{\hbar} \right)^2 \quad (2.17)$$

$$\beta_2 = (m+1) \left[-\frac{2m^* \alpha \rho}{\hbar^2} + (m+1) + \frac{eB}{\hbar^2} \rho^2 \right] \quad (2.18)$$

$$\lambda_2 = \frac{6m^* \rho^2}{\hbar^2} + \frac{m^* g \mu_B B \rho^2}{\hbar^2} + \frac{e \alpha m^* \rho^3 B}{\hbar^3} - \frac{1}{4} \left(\frac{eB \rho^2}{\hbar} \right)^2 \quad (2.19)$$

The solution of Eq. (2.11) can be determined by setting the determinant of the matrix equal to zero (See appendix A); therefore, the energy spectrum can be found as:

$$E_{1,2} = \frac{\hbar^2}{4m^* \rho^2} (2k_z^2 \rho^2 - \lambda_1 - \lambda_2 + \beta_1 + \beta_2) \pm \frac{1}{4} \sqrt{(4k_z \alpha)^2 + \frac{\hbar^4}{m^{*2} \rho^4} (\lambda_1 - \lambda_2 - \beta_1 + \beta_2)^2} \quad (2.20)$$

Where \pm is the branch – splitting quantum index. Spin up and down, respectively.

2.3. Magnetization and Susceptibility of the QD:

Magnetization is characterized by how magnetic materials are affected and responds to the magnetic field, and it can be evaluated by taking the first

derivative of the statistical average energy, Eq. (2.6), with respect to magnetic field as follow:

$$\begin{aligned} M(n_r, m, n_z, \omega_c, L, U_o) \\ = - \frac{\partial \langle E(n_r, m, n_z, \omega_c, L, U_o) \rangle}{\partial B} \end{aligned} \quad (2.21)$$

Where $\langle E_{n_r, m, n_z}(\omega_c, U_o, L, m, n_z, n_r) \rangle$ is average energy, which can be calculated by using the standard statistical definition:

$$\begin{aligned} \langle E_{n_r, m, n_z}(\omega_c, U_o, L, m, n_z, n_r) \rangle \\ = \frac{\sum_{n=1}^N E_{n_r, m, n_z}}{\sum_{n=1}^N e^{-\frac{E_n}{K\beta T}}} e^{-\frac{E_n}{K\beta T}} \end{aligned} \quad (2.22)$$

And for Eq. (2.20):

$$\begin{aligned} M(m, \rho, B, \alpha_R, k_z) \\ = - \frac{\partial \langle E(m, \rho, B, \alpha_R, k_z) \rangle}{\partial B} \end{aligned} \quad (2.23)$$

$$\begin{aligned} \langle E_m(m, \rho, B, \alpha, k_z) \rangle \\ = \frac{\sum_m^N E_m}{\sum_m^N e^{-\frac{E_m}{K\beta T}}} e^{-\frac{E_m}{K\beta T}} \end{aligned} \quad (2.24)$$

Susceptibility χ shows whether the material is attracted to the magnetic field, so it will be positive sign ($\chi > 0$) and it's called paramagnetic material or it will be repulsive to the magnetic field ($\chi < 0$), so it's called diamagnetic material . χ can be calculated from M using the following relation, [35].

$$\chi = \frac{\partial M}{\partial B} \quad (2.25)$$

2.4 Heat Capacity and Entropy:

Heat Capacity is defined as the amount of heat that is required to raise the material's temperature by (1°C) one degree, and it's the derivative of the average energy with respect to temperature[24],

$$C_v = \frac{\partial \langle E \rangle}{\partial T} \quad (2.26)$$

Entropy of a system depends on the number of possible microstate for the system and its partition function which is giving information about the configuration and arrangement of the locations and energies of the atoms or molecules that involve a system like the following:

$$S(T, \rho, B, \alpha_R, k_Z) = \frac{\partial (K_\beta T \ln \langle Z(T, \rho, B, \alpha_R, k_Z) \rangle)}{\partial T} \quad (2.27)$$

Where $Z(T, \rho, B, \alpha_R, k_Z) = \sum_{j=1}^{jmax} e^{-\frac{E_j}{k_\beta T}}$ is the partition function of the system.

Chapter Three

Results and Discussions

Our computed results are presented into two parts. In the first part, we will discuss the obtained results for the energy spectra of an electron confined in a GaAs cylindrical QD under external magnetic field and confining potential in radial dimension and pseudo harmonic potential in z-direction without Rashba effect and Zeeman term.

In the second part, we will discuss the obtained result for the energy spectra of an electron confined in InAs cylindrical quantum dot under external magnetic field and Rashba Spin -orbit interaction with Zeeman term.

3.1 GaAs Cylindrical QD with Zero Rashba Effect:

We study the physical properties of the GaAs QDs material by computing the statistical energy, magnetization, susceptibility and heat capacity.

For GaAs QD, we used the following physical parameters:

Effective electron mass: $m^* = 0.067m_e$

Effective Rydberg energy: $R^* = 5.694 \text{ meV}$

Effective Bohr radius: $a^* = 9.8 \text{ nm}$

Magnetic field dependent cyclotron frequency $\omega_c(R^*) = 0.296 \times (B \text{ in Tesla } (T))$

3.1.1 Quantum Dot Spectra and Statistical Energy:

In this section, we present our computed results for confining energies of an electron confined in a cylindrical quantum dot under the radial potential, pseudo harmonic potential and external magnetic field, for different ranges of physical parameters.

Table 3.1: The values of the ground state energy, with changing angular quantum number m from $-1 \rightarrow 1$ and the radial quantum number n is taken from $0 \rightarrow 1$, at $\omega_0=5\text{meV}$, $B=1$ Tesla, $L=5$ nm and $U_0 = 3\text{meV}$.

$\{n_r, n_z, m\}$	Energy in (meV)
{0,0,0}	7.44729
{0,1,0}	10.72924
{0,0,-1}	11.68990
{0,0, 1}	13.33990
{0,1,-1}	14.97185
{0,1,1}	16.62185
{1,0,0}	17.58250
{1,1,0}	20.86446
{1,0,-1}	21.82511
{1,0,1}	23.47511
{1,1,-1}	25.10706
{1,1,1}	26.75706

In Figure (3.1), we have plotted binding energy against B . the figure shows that the binding energy increases as B increases. This is an expected behavior; due to the presence of an external magnetic field, which adds new confinement term to the electron as seen from Hamiltonian equation (2.1), also the figure shows energy level crossing.

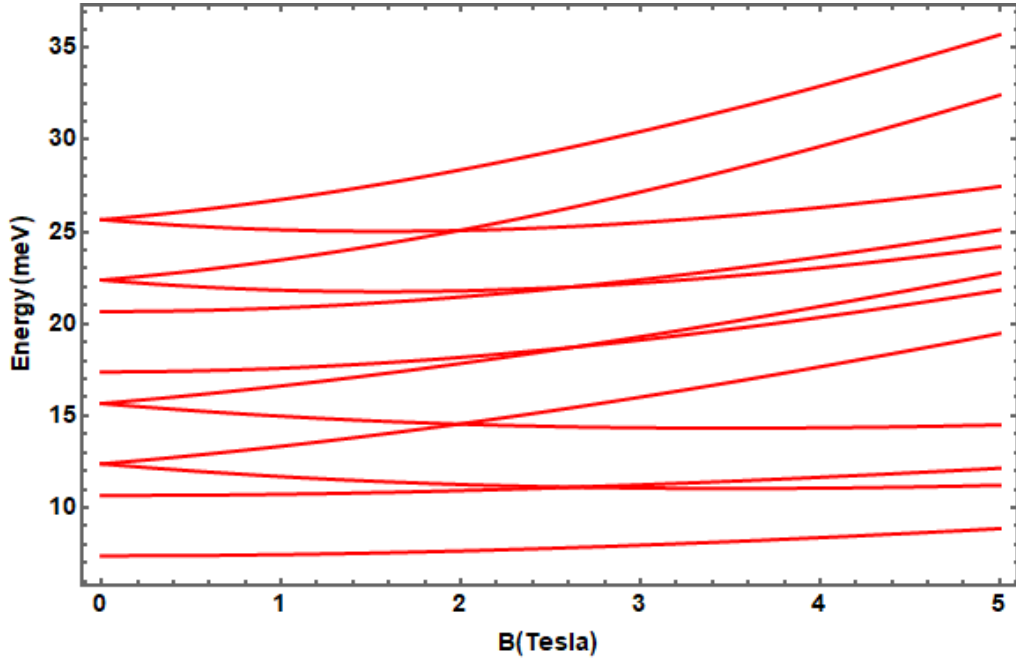


Fig. 3.1: The energy spectra of an electron at $\omega_0 = 5\text{meV}$, $U_0 = 3\text{meV}$, $L=5\text{nm}$, $n_r(0 \rightarrow 1)$, $n_z(0 \rightarrow 1)$, and $m(-1 \rightarrow 1)$.

3.1.2 Convergency Test and Statistical Energy:

The first and important step in our work is to ensure the convergency of the statistical average energy of the QD. To achieve this goal, we plot in Fig.3.2, the statistical energy using equation (2.22) as function of number of basis for various set of temperatures.

Fig. (3.2) shows the statistical energy $\langle E \rangle$ calculated by taking quite large number of basis: $n_r(0 \rightarrow 15)$, $n_z(0 \rightarrow 15)$ and $m(-25 \rightarrow 25)$. For low temperature range ($T=30$ and 50 K), a small number of basis ($\sim \#200$) is enough, however, a large number of basis is needed ($\sim \#800$) for temperature $T=180$ K. The number of choices $\#800$ is a good choice, as indicate by the vertical line shown in the plot.

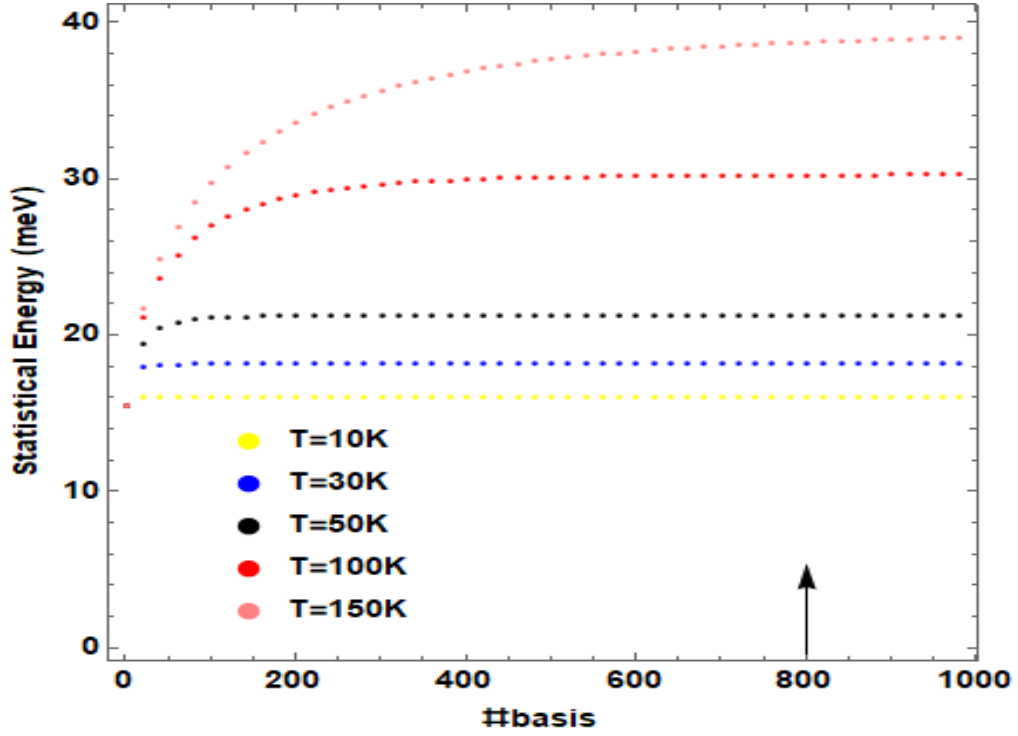


Fig3.2: Statistical average energy Vs. #basis calculated at different values of T, at $\omega_0 = 4\text{meV}$, $B = 10\text{Tesla}$, $U_0 = 15\text{meV}$, and $L = 5\text{nm}$.

To investigate the effects of external parameters like temperature, ω_0 and U_0 , we have plotted in Fig. (3.5) the Statistical average energy against B at $\omega_0 = 5\text{meV}$, $L = 5\text{nm}$ and $U_0 = 10\text{meV}$.

When the magnetic field is increased, the $\langle E \rangle$ increases too, and this resulting from the additional confinement of the electron by the external magnetic field, and for different values of temperature, the figure shows that the statistical energy is enhanced for higher temperature.

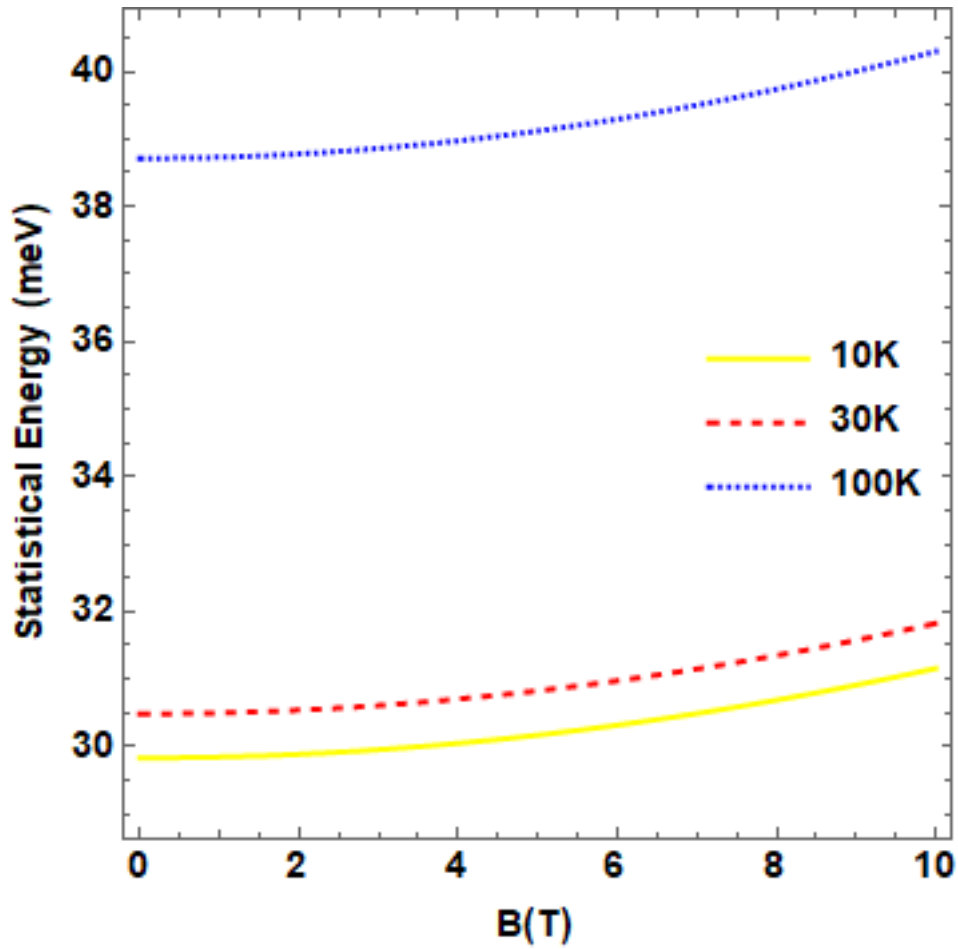


Fig.3.3: Statistical average energy against B for different values of T (T= 10 K for solid line, =30 K for dashed line=100K for dotted line). At $L=5\text{nm}$, **and** $U_0 = 5\text{meV}$.

Fig. 3.4 shows the effect of the strength of the confinement frequency (ω_0) on the behavior of $\langle E \rangle$. The figure displays a large change on the behavior of the energy curves as result of raising ω_0 from 4meV to 12meV, because of large energy confinement. The figure shows also that B has more effect on statistical average energy at low temperature.

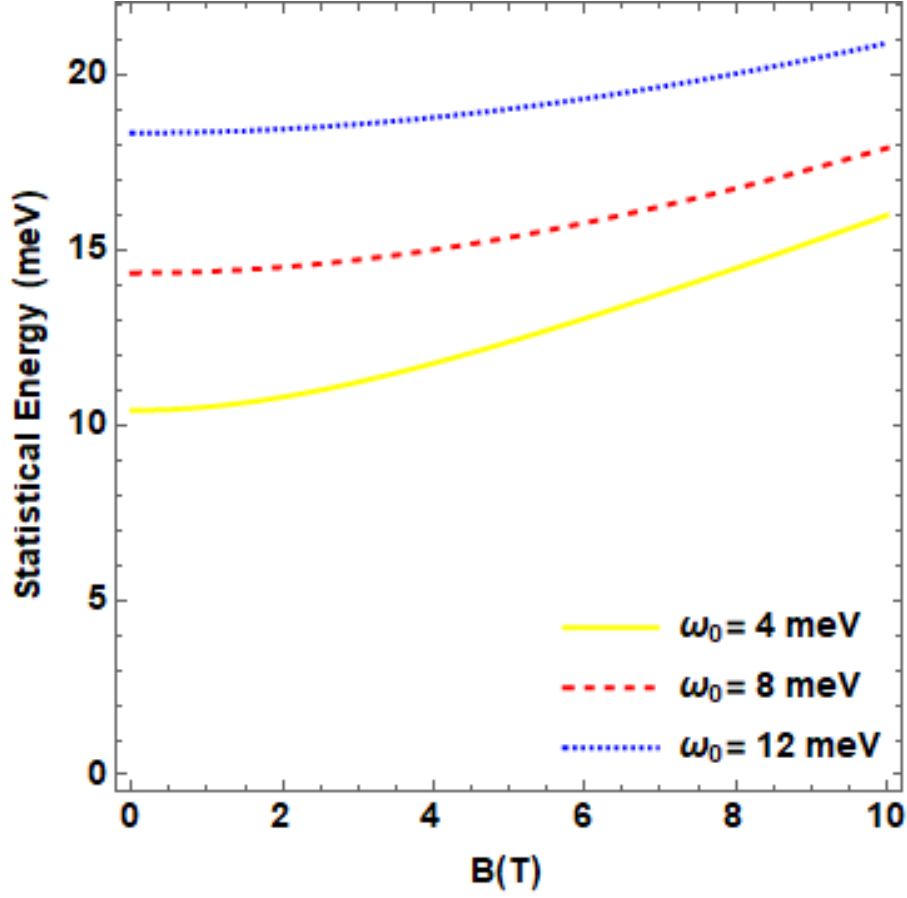


Fig. 3.4: Statistical average energy as a function of external magnetic field for three different values of ω_0 ($\omega_0 = 4\text{meV}$ for solid line, 8meV for dashed line, and 12meV for dotted line). At $T = 10\text{K}$, $L = 5\text{nm}$, and $U_0 = 5\text{meV}$.

In Fig (3.5), we have plotted statistical energy vs. B (T) for different pseudo potential strength U_0 . The figure shows that as U_0 increases the statistical energy increases also due to further confinement of the electron which enhances the average energy.

The effect of confining length on the energy of the system is shown in Fig (3.6). The figure shows that increasing the confining length (L) of the QD leads to a reduction in the energy due to inverse proportional of E with L, and the electron becomes less confined as L increases.

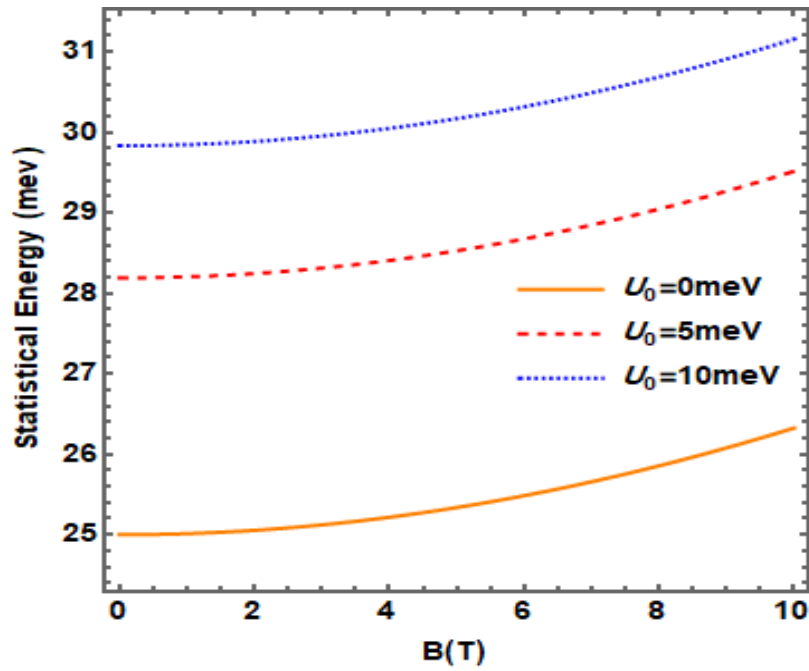


Fig.3.5: Statistical average energy as function of external magnetic field for three different values of pseudo potential strength U_0 ($U_0 = 0\text{meV}$ for solid line, 5meV for dashed line, and 10meV for dotted line). At $T = 10\text{K}$, $L = 5\text{nm}$, and $\omega_0 = 25\text{meV}$.

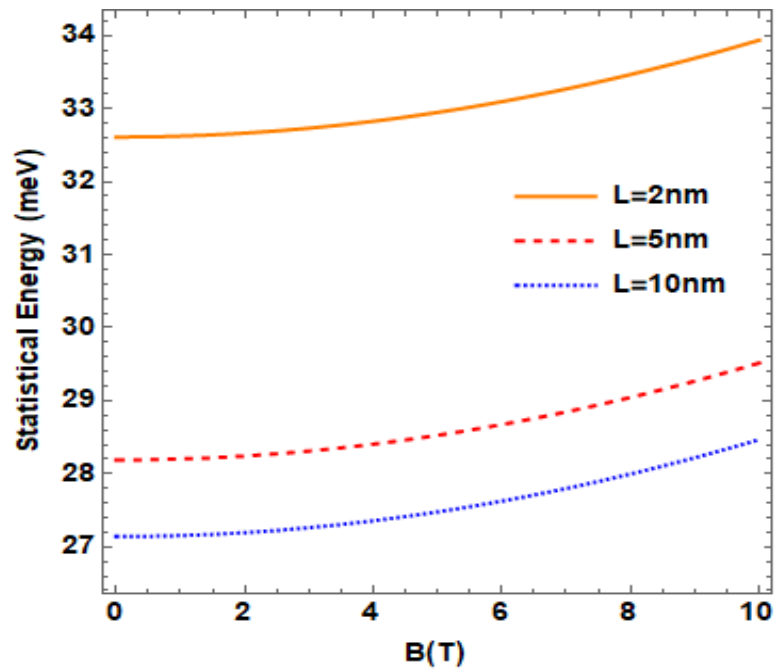


Fig.3.6: Statistical average energy against B for different values of L ($L = 2\text{nm}$ for solid line, $= 5\text{nm}$ for dashed line, $= 10\text{nm}$ for dotted line). At $T = 10\text{K}$, $U_0 = 5\text{meV}$, and $\omega_0 = 25\text{meV}$.

3.1.3 Heat Capacity:

In this section, we will show the effects of T , B and U_0 on the heat capacity by substituting eq. (2.6) in eq. (2.26) to get a relation between them.

We have presented in Fig 3.7 the heat capacity C_v of a QD as a function of temperature for three different values of magnetic field $B = 0$ T, 5T, and 10 T.

At the beginning, when the temperature is increased from absolute zero, C_v suddenly increases and then decreases giving a peak-like structure, [34]. This observed peak structure is the well-known Schottky - anomaly of the heat capacity, and this phenomenon which is subjected to a system with only two states is important, because at low temperature the thermal energy gained by the electron as kinetic energy is enough for only exciting the electron from the ground state to the first excited state.

As the temperature increased more and more, the heat capacity starts increasing almost linearly and converges to the saturation value of $2k_B$. The increasing of heat capacity is steady and this is due to the increase in thermal energy $k_B T$ of electrons as the temperature is increased which makes large number of states available for thermal excitations.

The figure shows also that as B is increased, the peak shifts to the right and become broad in width. The saturation value of the C_v , at a high temperature approaches about $2k_B$, in agreement with result reported in Ref.[21]

The specific heat capacity depends on the distribution of energy levels, temperature and the occupation probability of the states.

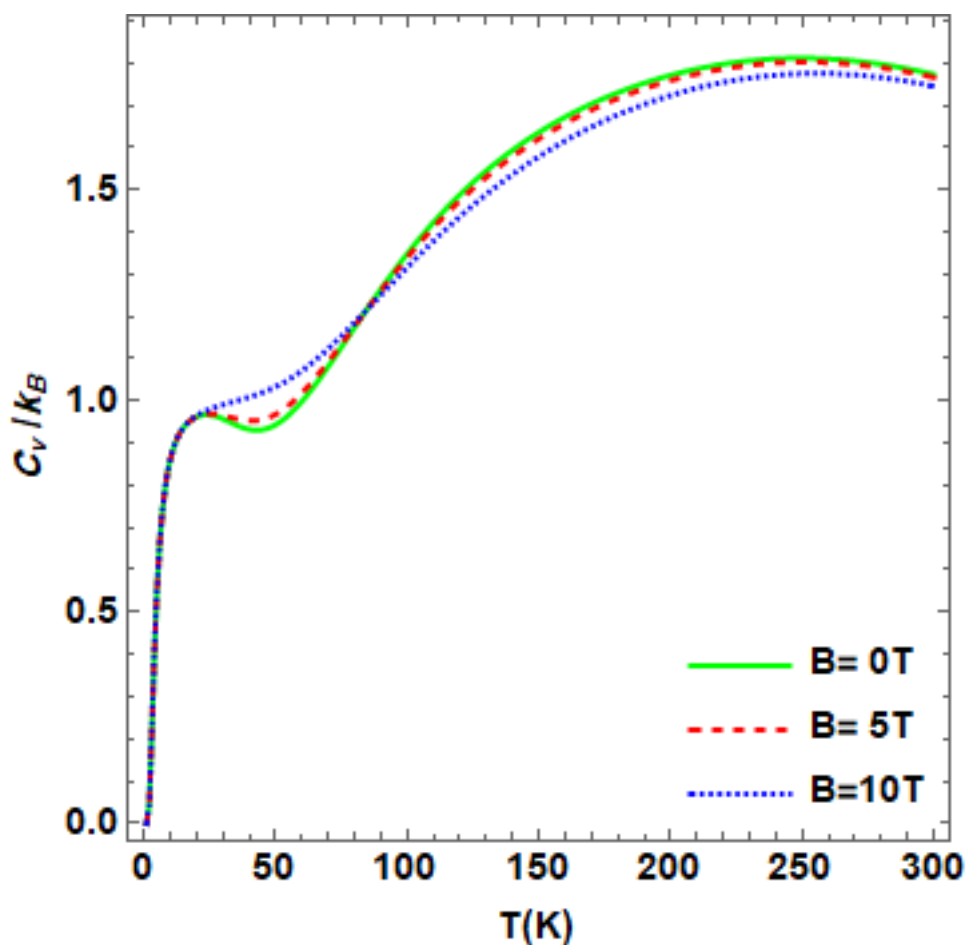


Fig.3.7: Variation of specific heat with temperature for different values of B (B = 0T for solid line, = 5T for dashed line, = 10T for dotted line). At $\omega_0=25\text{meV}$, $L=20\text{nm}$, and $U_0=6\text{nm}$.

Fig.3.8 shows the effect of the confinement Pseudo strength U_0 on $C_v - T$ curve by taking different values of U_0 at particular values of the quantum dot size R , and the magnetic field strength B .

From the figure, we can observe that at low temperatures the $C_v - T$ curve behaves qualitatively the same way for the three different U_0 values to reach the same peak- height which shifts to the right at large U_0 . The change in the heat capacity behavior starts in decreasing of the C_v after the peak, where we

notice that the larger the value of U_0 the lower the C_v value , after the peak, before it re-raises again, C_v starts increasing almost linearly and converges to the saturation value of $2k_B$. The obtained heat capacity limit-cases are consistent with the discussion given in Ref [21].

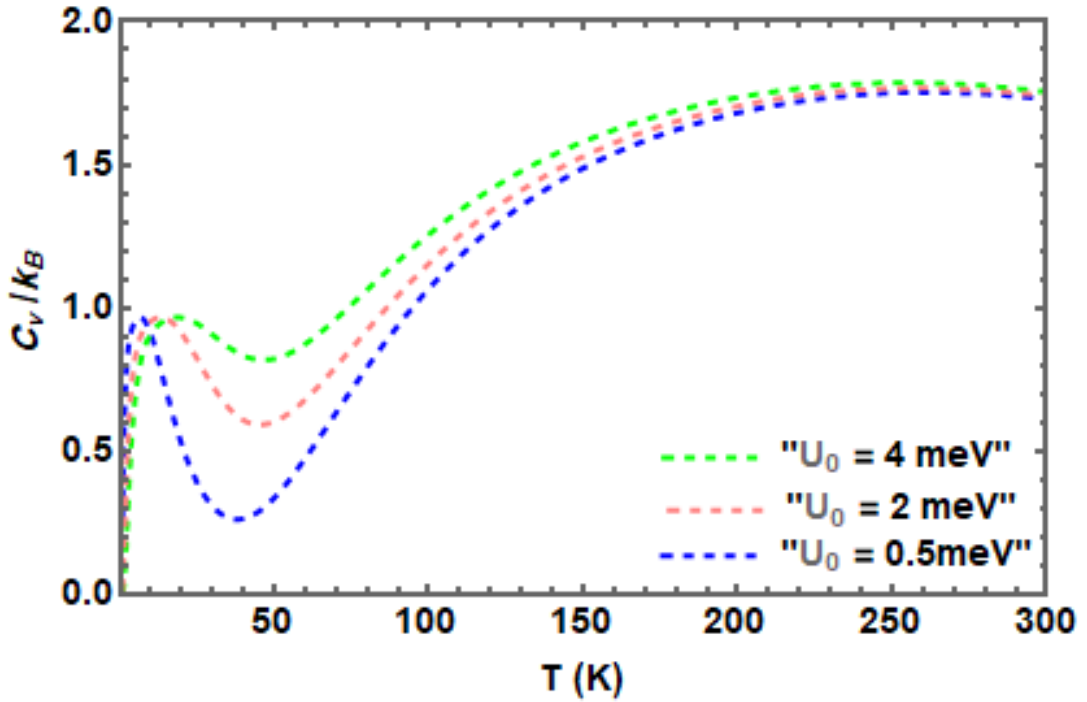


Fig.3.8: Variation of specific heat with temperature for different values of U_0 ($U_0 = 0.5, 2, 4 \text{ meV}$ from bottom to top). At $L=20\text{nm}$, $B=5\text{T}$, and $\omega_0 = 25\text{meV}$

3.1.4 Magnetization and Susceptibility:

In this section, we will present and discuss our computed results for the magnetization (M) and susceptibility (χ) of the GaAs QD as a function of different physical parameters.

After computing the statistical energy $\langle E \rangle$, we have calculated the magnetization M of GaAs/AlGaAs QD system by using equation (2.21).

Magnetization gives us the information about how the system interact with an external magnetic field.

In Fig 3.9, we have plotted the magnetization against B at different temperature values. The magnetization changes suddenly with a little increases in magnetic field. As we increase the magnetic field, the occupancy of a higher angular momentum state becomes energetically suitable, yield to the decreasing of magnetization.

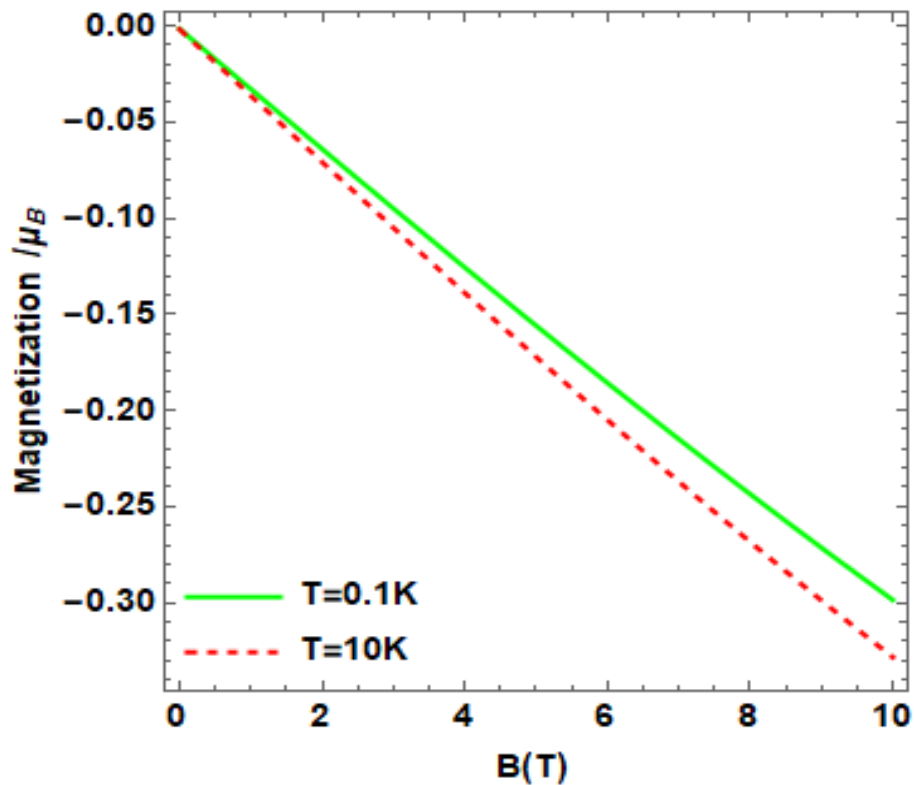


Fig.3.9: Magnetization (M) of GaAs quantum dot as a function of external magnetic field for two different values of T (T=0.1K for solid line, =10 K for dashed line). At $\omega_0 = 25$ meV, L=5nm, and $U_0 = 10$ meV

Susceptibility (χ) which is defined as how M changes with respect to B, is shown in Fig3.10. The Figure shows the behavior of the susceptibility as a function of the external magnetic field. It is obviously shown that the

susceptibility of ground state is diamagnetic for the present range of B (0-10) T.

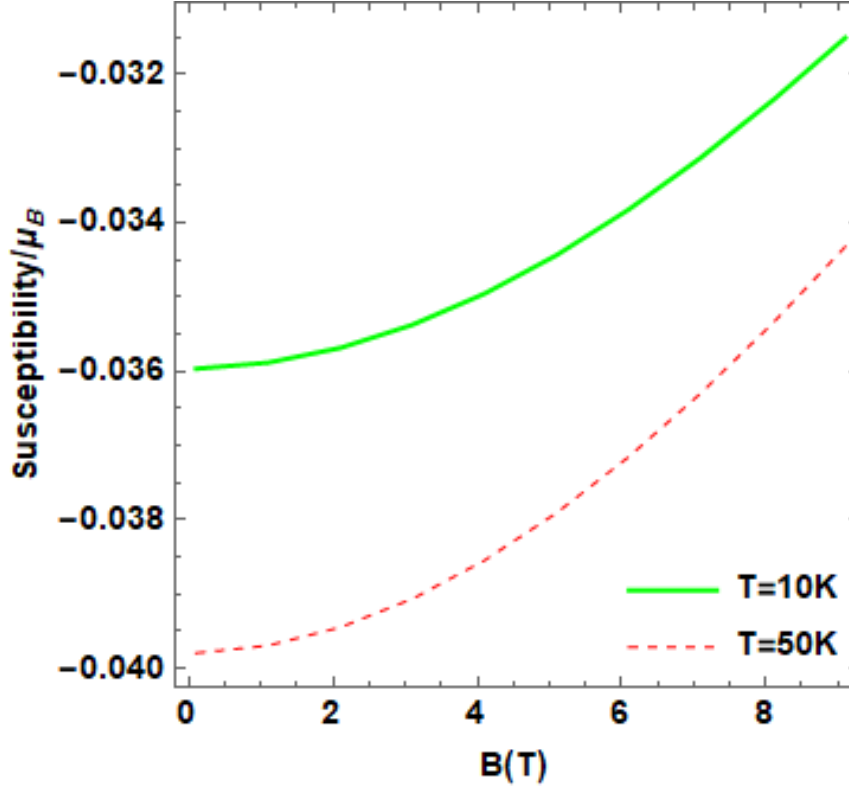


Fig. 3.10: Magnetic susceptibility (χ) of GaAs quantum dot as a function of external magnetic field for two different values of T (T=10K for solid line, =50 K for dashed line). At $\omega_0 = 25$ meV, $L=5$ nm and $U_0 = 10$ meV.

The variation of magnetization (M) with temperature (T) at $L=5$ nm, $U_0=5$ meV and $\omega_0=25$ meV is shown in figure 3.11, from the figure we can observe that the magnetization is not affected by increasing the temperature until it reaches $T=30$ K, after that there is a decreasing in M, and M is large for low B, this indicates that the material is diamagnetic.

In addition, Figure 3.12 shows the variation of susceptibility with temperature at $L=5$ nm, $U_0 = 5$ meV and confining frequency = 25meV. The

susceptibility does not vary by increasing the temperature until $T=25\text{k}$, after that it decreasing linearly, for both values of magnetic field $B=5$ and 10T .

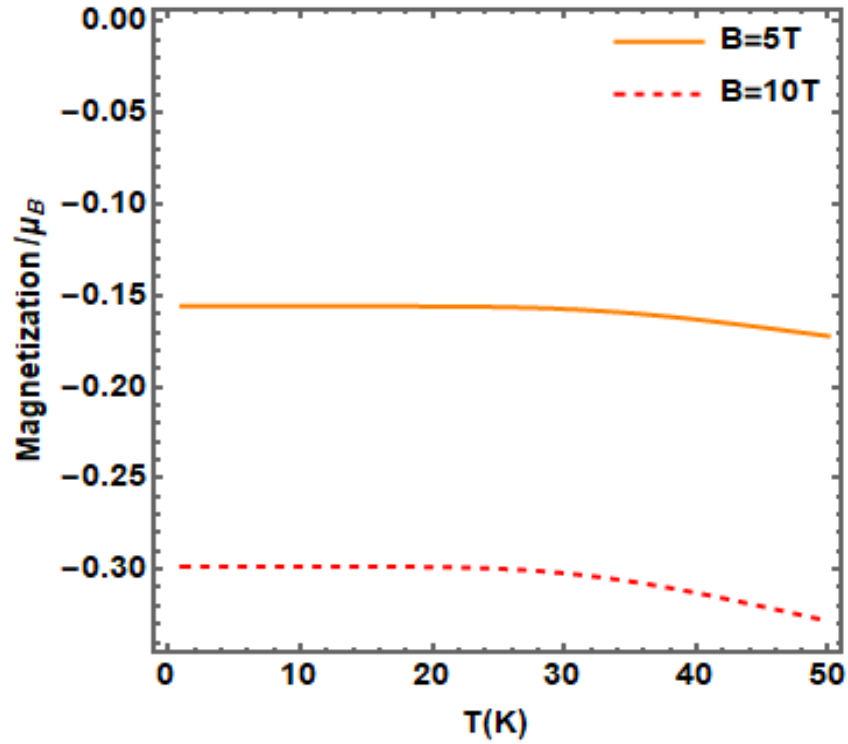


Fig.3.11: Magnetization (M) of GaAs quantum dot as a function of temperature for two different values of **magnetic field** ($B=5\text{T}$ for solid line, $=10\text{T}$ for dashed line) .At $T = 10\text{K}$, $L=5\text{nm}$ and $\omega_0 = 25\text{meV}$.

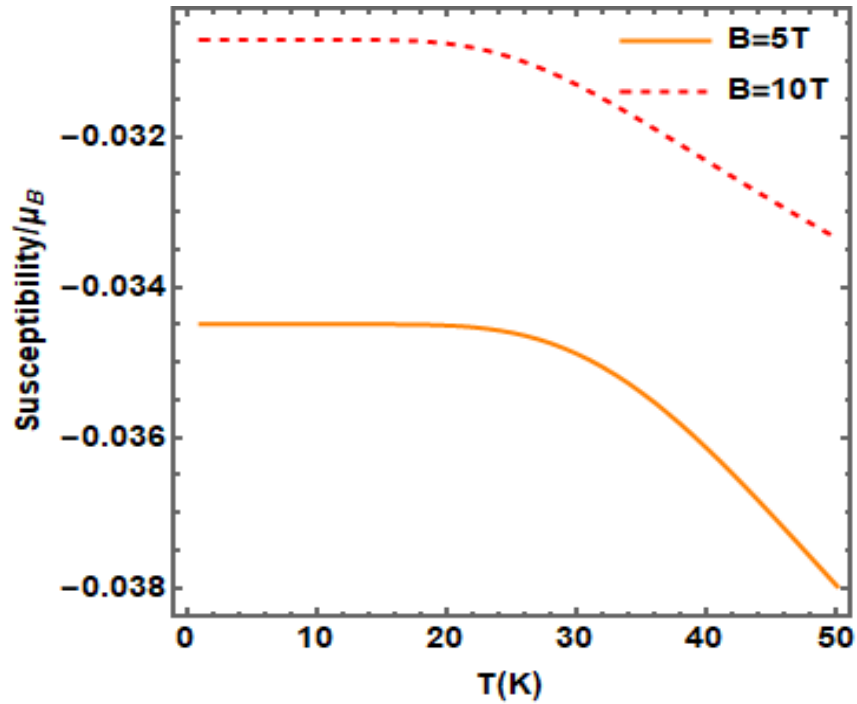


Fig.3.12: Magnetic Susceptibility (χ) of GaAs quantum dot as a function of temperature for two different values of **magnetic field**($B=5\text{T}$ for solid line, $=10\text{T}$ for dashed line)

.At $T = 10\text{K}$, $L=5\text{nm}$ and $\omega_0 = 25\text{meV}$.

The effect of the confining frequency (ω_0) on M and χ have plotted in fig 3.13 and 3.14, respectively, at $L=5\text{nm}$, $U_0 = 15\text{meV}$ and $T=10\text{K}$.

From figure (3.13), the magnetization is large for high confining frequency, and for all values of confining frequency, the magnetization decreases as the magnetic field increases.

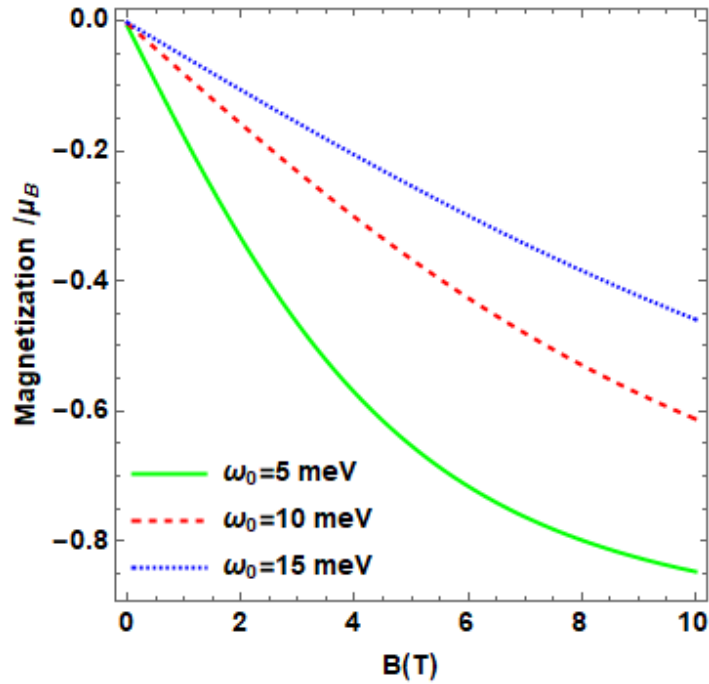


Fig.3.13: Magnetization (M) of GaAs quantum dot as a function of external magnetic field for three different values of ω_0 ($\omega_0=5\text{meV}$ for solid line, $=10\text{meV}$ for dashed line, $=15\text{meV}$ for dotted line) .At $T = 10\text{K}$, $L=5\text{nm}$ and $U_0 = 10\text{meV}$.

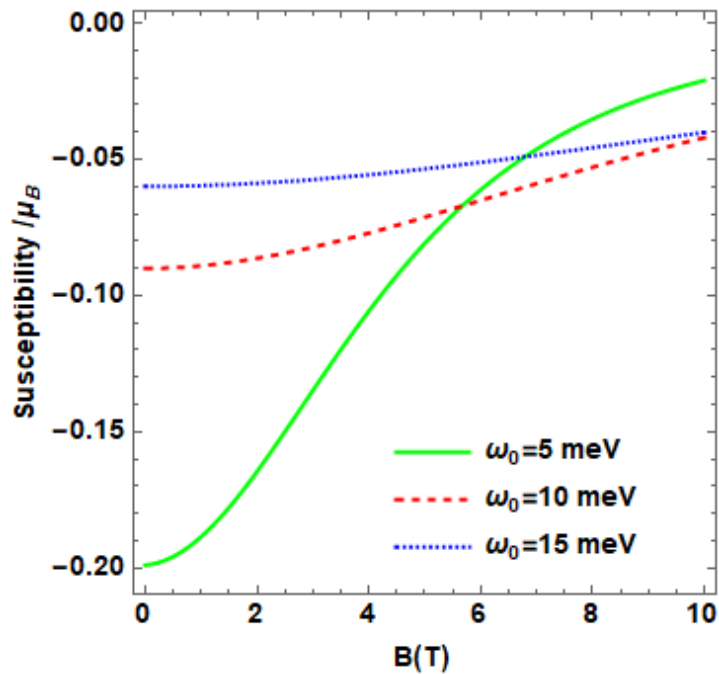


Fig3.14: Magnetic susceptibility (χ) of GaAs quantum dot as a function of external magnetic field B for three different values of ω_0 ($\omega_0=5\text{meV}$ for solid line, $=10\text{meV}$ for dashed line, $=15\text{meV}$ for dotted line) .At $T = 10\text{K}$, $L=5\text{nm}$ and $U_0 = 10\text{meV}$.

Figure .3.14 shows that as the confinement frequency increases ($\omega_0 = 15meV$), the susceptibility become independent of the magnetic field because of the domination of the confining potential strength.

3.2 InAs - Cylindrical QD with Rashba Effect:

In this section, we will analyze the computed results for the energy spectra of an electron confined in a cylindrical QD under external magnetic field and SOI with Zeeman term.

We study the physical properties of the InAs QDs material by computing the magnetic and thermal quantities like statistical energy $\langle E \rangle$, magnetization (M), susceptibility (χ), heat capacity (C_v) and entropy (S).

For InAs QD, we used the following material parameters:

We used the effective electron mass: $m^* = 0.042 m_e$, effective Rydberg energy: $R^* = 2.68 meV$, effective Bohr radius: $a^* = 18.39 nm$, magnetic field frequency relation $\omega_c: (\omega_c(R^*) = 0.296 \times (B \text{ in Tesla } (T)))$, and effective Lande g-factor ($g^*) = -14$.

3.2.1 Energy Spectrum and Statistical Energy:

Computation of the energy spectra is an essential step in studying the thermo-magnetic properties of the nanomaterial's QD. In this section, we explain the thermodynamic and magnetic properties presented by a QD in the presence of B and RSOI.

The plan is; first, to calculate the energy spectrum of the quantum dot system. Second, use the statistical average energy to find its magneto-thermodynamic behavior. Finally, we discuss the properties of a cylindrical QD formed out of a three-dimensional heterostructure in which it is assumed that electrons are strictly confined at the surface of the cylinder, [36].

Fig 3.15 shows the effect of the presence of Zeeman term on energy spectra as function of the magnetic field strength B in the ground state $m=0$, $\rho = 8nm$, and $k_z = 0$, solid (dashed) line is for the spin $= \frac{1}{2}$ (zero values). The figure shows the crossing between the energy levels and the change in the angular momentum of the ground state. As the magnetic field increases, the spin and Zeeman terms show considerable energy contribution effects. The plot shows also the splitting in energy level as a result of interaction of the magnetic field with the spin of the electron, [Zeeman effect].

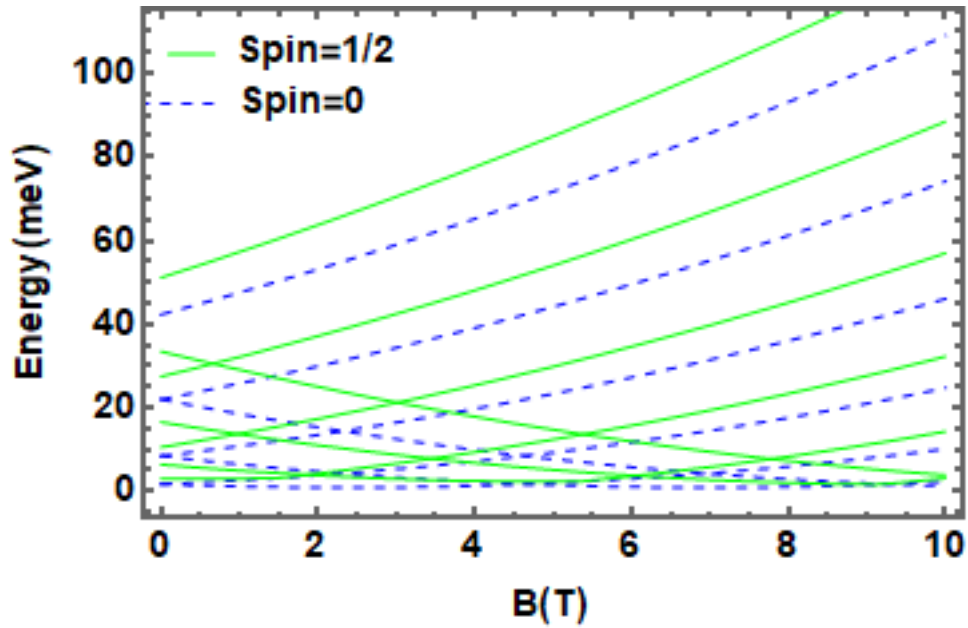


Fig. 3.15: The calculated energies of a single electron QD versus the magnetic field at $\rho=10$ nm and $\alpha_R = 0$ meV.nm. The solid (dashed) curves for $S = \frac{1}{2}$ (0), respectively.

To show the effect of the RSOI on the QD spectra, we have plotted in Fig 3.16 the energy against B (T) with and without Rashba parameter. The figure shows shifting and decreasing in the energy levels in the presence of Rashba parameter. The Rashba term acts like electric field effect on electron, name as [stark effect] tends to separate the electron, i.e. It moves the electron away, increasing the distance between the electron and the nucleus, which results in decreasing the confinement and the Coulomb interaction, and hence decreasing the binding energy. The interesting result of the energy levels crossing clearly appears as oscillating peaks in the magnetic quantities, which will be presented later.

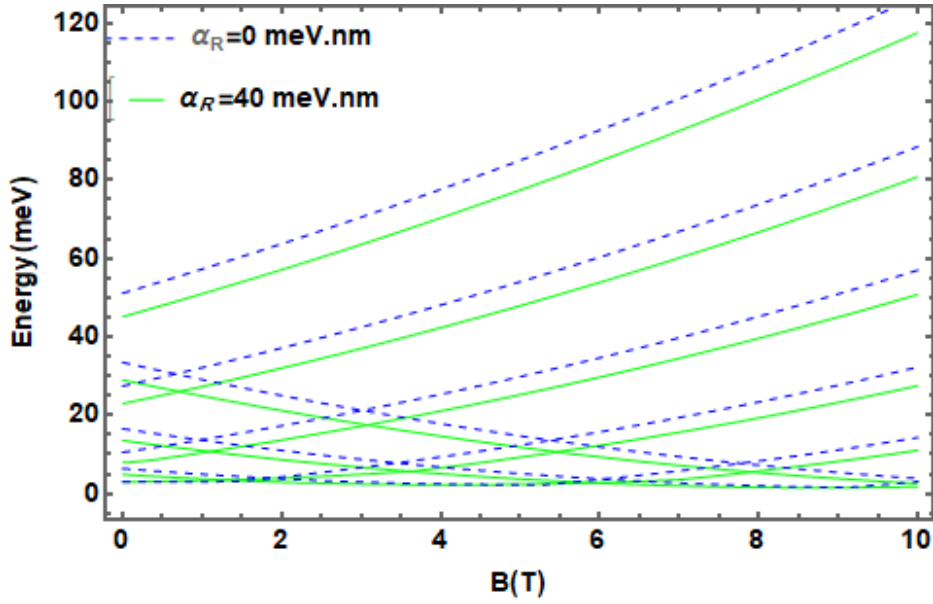


Fig.3.16: Confinement energy as a function of magnetic field, for two different values of RSOI parameter α_R ($\alpha_R = 40\text{meV.nm}$ for solid line, $= 0\text{ meV.nm}$ for dashed line). At $\rho=10\text{nm}$.

Figure 3.17 describes the statistical energy $\langle E \rangle$ as a function of the magnetic field B of the QD, in the presence of the effect of the electron spin term. The figure shows that at low temperature, $T= 0.1\text{K}$, the energy goes down as B increases, since the contribution of the thermal energy is small at low B , this behavior continues up to $B \approx 1\text{ T}$, then the energy begins to increase as the magnetic field raises.

When the temperature is increased, from 0.1K to 10 and 20 K , respectively, the curve of the ground state shows a significant enhancement due to the considerable increase in the contribution of the thermal energy, [34]. The curves show oscillating behavior which is attributed to the energy levels crossings in the QD spectra.

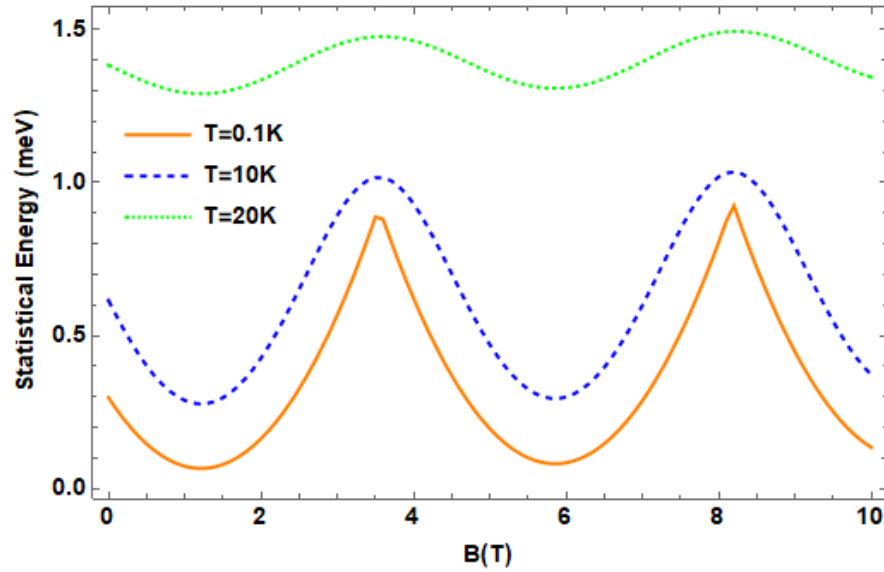


Figure. 3.17: The statistical energy against the magnetic field B for three different values of T ($T = 0.1$ K, 10, and 20 K from bottom to top). At $\alpha_R=10$ meV.nm, $\rho=10$ nm.

3.2.2 Magnetization and Susceptibility of InAs – QD:

We also investigated here the effect of B on the magnetization (M) and susceptibility (χ). M gives us the information about how the system interact with B . When RSOI turned off ($\alpha_R = 0$), magnetization changes suddenly with the increase in B , and it starts decreasing.

At a certain value of magnetic field, M becomes equal to zero and the addition increase in magnetic field causing change in the sign of M . Thereby, a magnetic phase transition occurs and the material changes from Diamagnetism ($\chi < 0$) to Paramagnetism ($\chi > 0$). The M -curves shows a peak structure, which results from the transition of the angular momentum of the ground state energy as shown before in Fig 3.15.

From Fig 3.18, we noticed that as the temperature is increased, the heights of the peaks due to transition jumps are reduced, broadened and shifted to higher magnetic field value.

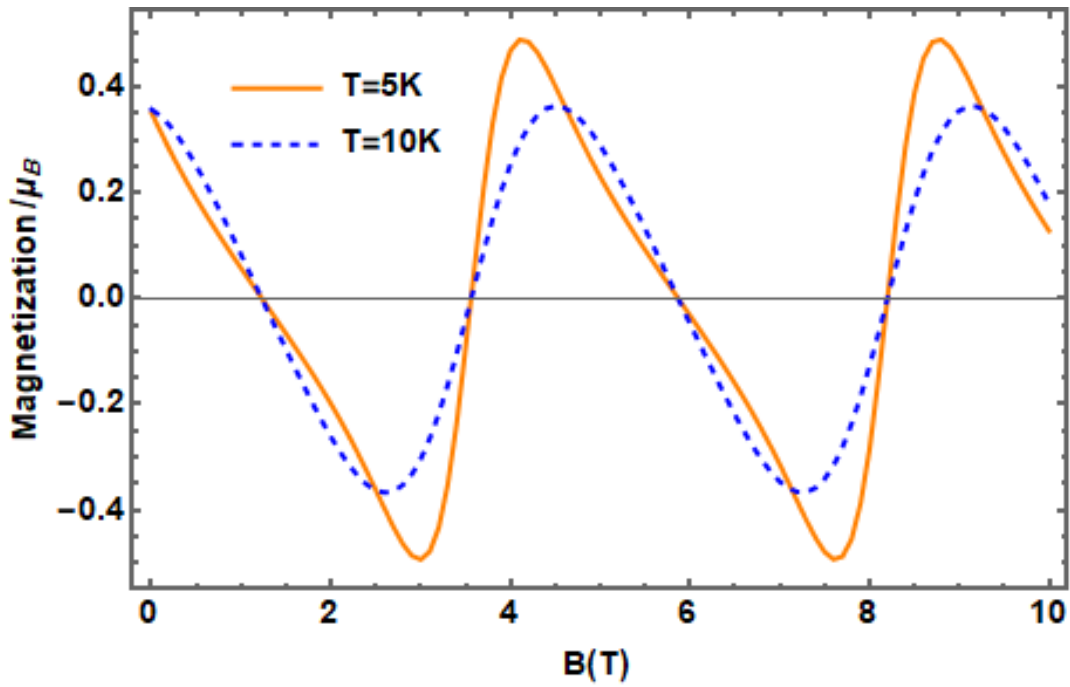


Fig.3.18: Magnetization (M) of InAs quantum dot as a function of external magnetic field for two different values of T ($T=5\text{K}$ for solid line = 10K for dashed line) .At $\rho=10$ nm, $\alpha_R=10$ meV.nm.

The first peak related to the transition in the angular momentum from $m=0$ to $m=1$, in the magnetic field strength range $B=(3-4)T$.

Susceptibility, which is related to the first derivative of M with respect to B , is shown in Fig.3.19.

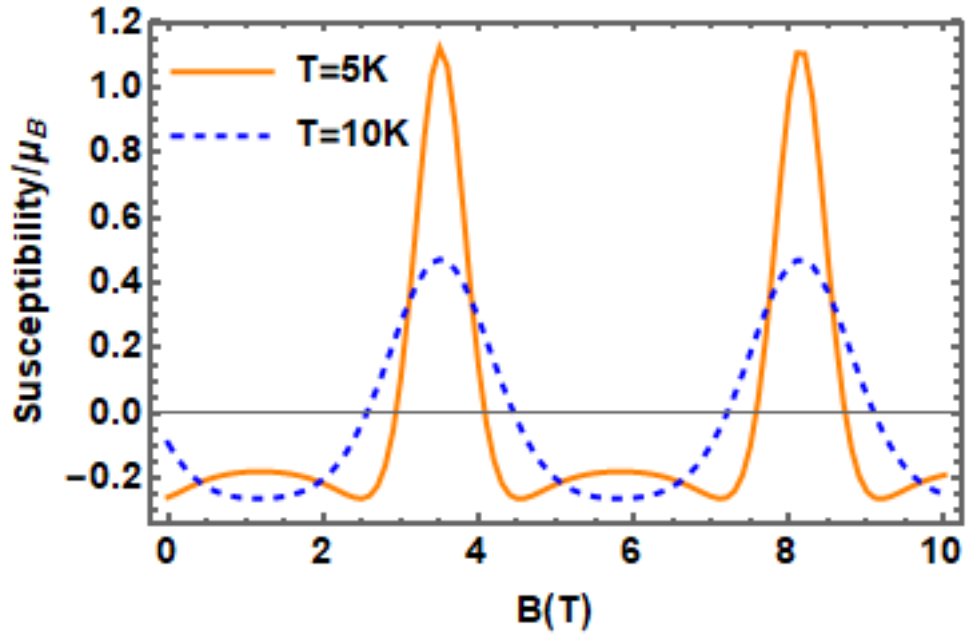


Fig.3.19: Magnetic susceptibility (χ) of InAs as a function of external magnetic field for two different values of T (T=5K for solid line = 10K for dashed line). At $\rho= 10\text{nm}$, and $\alpha_R= 10\text{meV.nm}$.

Hence, in fig .3.18 the material at these peaks changed its magnetic state from diamagnetic to paramagnetic at low magnetic fields and to diamagnetic again.

To investigate the effect of RSOI on the magnetization, we have displayed in Fig.3.20 the (M) against B for zero and non-zero Rashba parameter strength. The figure shows that for $\alpha_R = (40\text{meV.nm})$ it shifts the peaks towards higher magnetic field.

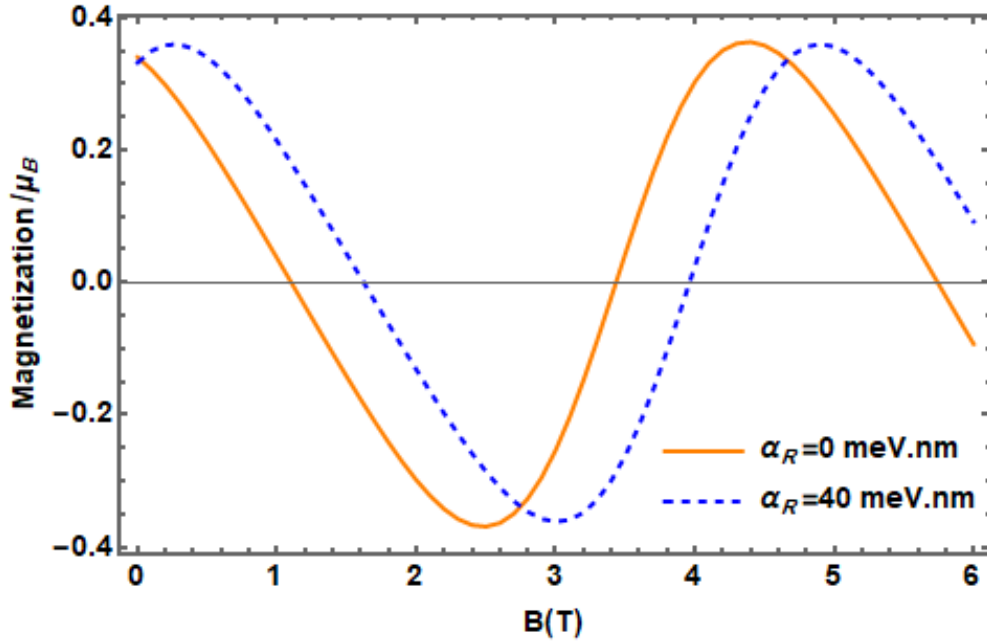


Fig.3.20: Magnetization (M) of InAs quantum dot as a function of external magnetic field for two different values of Rashba parameter ($\alpha_R = 0$ meV·nm for solid line $\alpha_R = 40$ meV·nm for dashed line). At $\rho = 10$ nm, and $T = 10$ K.

Susceptibility χ which is known as the rate of change of M with respect to B is shown in Fig.3.21. The effect of RSOI is shown on χ -curve at low magnetic field strength range $B = (0-10)$ T.

Fig. 3.21 shows the susceptibility behavior as a function of external magnetic field. From the figure we can notice that the material changes its behavior from negative (χ) (Diamagnetic material) to positive χ (Paramagnetic material) at ($B = 5T$) and it returns again to Diamagnetic at ($B = 7T$), And the peak shifts toward high magnetic field in the presence of Rashba parameter $\{\alpha = 40 \text{ meV} \cdot \text{nm}\}$.

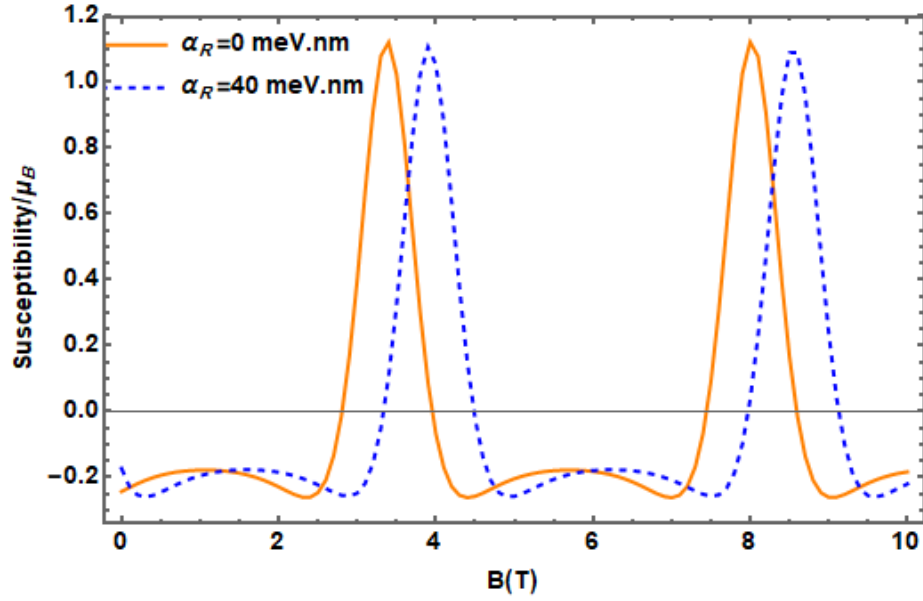


Fig.3.21: Magnetic susceptibility (χ) of InAs quantum dot as a function of external magnetic field for two different values of Rashba parameter ($\alpha_R = 0 \text{ meV}\cdot\text{nm}$ for solid line, $\alpha_R = 40 \text{ meV}\cdot\text{nm}$ for dashed line) .At $\rho = 10 \text{ nm}$, and $T = 10 \text{ K}$.

The variation of M with Rashba spin orbit interaction parameter has plotted in Fig3.22 .The plot shows that the magnetization M increase as α_R increases, and that the magnetization is large for high magnetic field.

Also the variation of χ with Rashba spin orbit interaction parameter is plotted in Fig3.23.The figure shows that the susceptibility χ increase as α_R increases, and that the χ is large for high magnetic field.

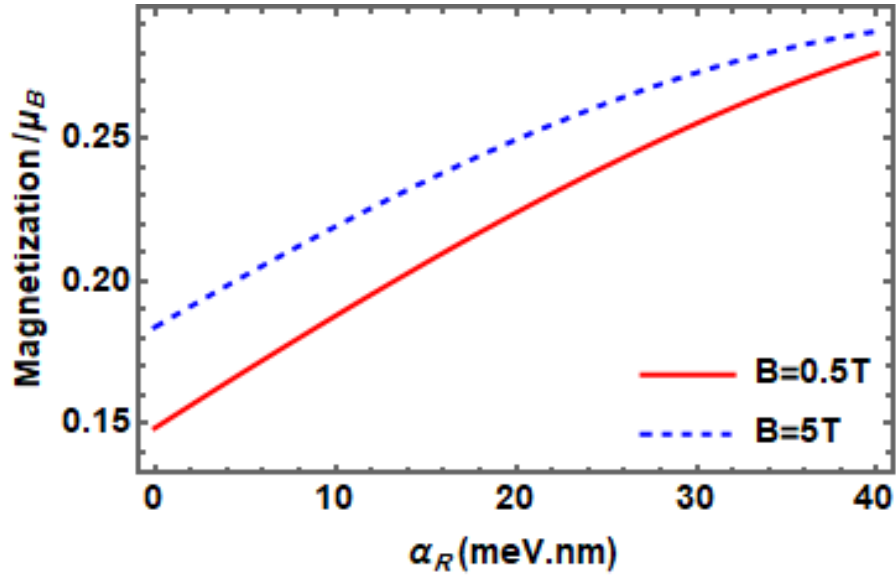


Fig.3.22: Magnetization (M) of InAs quantum dot as a function of RSOI parameter for two different values of magnetic field strength B ($B = 0.5$ T for solid line, $B=5$ T for dashed line) .At $\rho=10\text{nm}$ and $T=10\text{K}$.

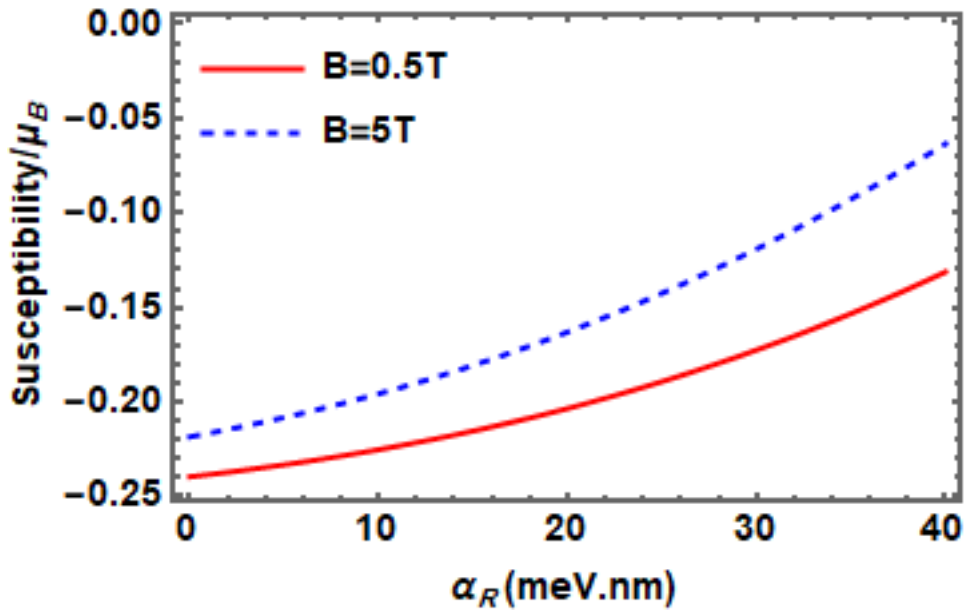


Fig.3.23: Magnetic susceptibility (χ) of InAs quantum dot as a function of RSOI parameter for two different values of magnetic field strength B ($B = 0.5$ T for solid line, $B=5$ T for dashed line) .At $\rho=10\text{nm}$ and $T=10\text{K}$.

3.2.3 Heat Capacity:

In Fig. 3.24, we have presented the computed heat capacity C_v , of a QD as a function of temperature for three different values of Rashba parameter $\alpha_R = 0, 20$ and 40 meV.nm at $\rho = 10$ nm, and $B = 5$ T. For all values of RSOI parameter, the heat capacity almost approaches to zero as T goes to zero. When the temperature is increased from absolute zero, C_v suddenly increases and then decreases giving a peak-like structure. Sharpness and shifting of the peak to lower temperature occur due to the spin-orbit interaction. Since spin-orbit interaction removes the degeneracy of the spin, large number of energy level exists in the unit range of energy, and this yield to a reduction in the level spacing, and shifting the peak to lower thermal energy and therefore lower C_v . As the temperature increases more and more, specific heat starts to be temperature independent and converges to the saturation value of $\frac{1}{2}k_B$. Since the electron move freely at φ direction only, so it act like 1D motion, which give $\frac{1}{2}k_B$ for its degree of freedom, [37].

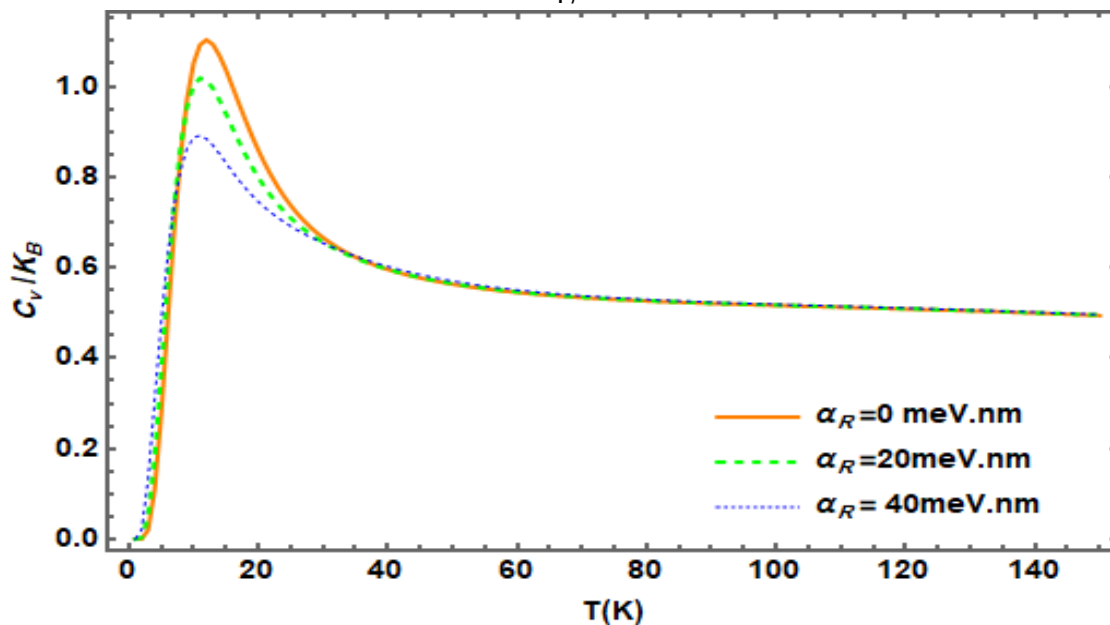


Fig .3.24: Variation of specific heat with temperature for different values of RSOI parameter α_R = (0meV.nm for solid line, 20meV.nm for dashed line, and 40meV.nm for dotted line). At $B=5$ Tesla, and $\rho=10$ nm.

In fig. 3.25, we have presented the computed specific heat values of a QD as a function of temperature for three different values of magnetic field strength B , $B= 0.5$ T, 2.0 T, and 5.0 T at $\rho=5$ nm, $\alpha=20$ meV.nm. At low magnetic field strength, the figure shows that when the temperature is increased from absolute zero, C_v suddenly increases and then decreases giving a peak-like structure. As the magnetic field increases, the spacing between the different Landau levels increases also, so the electron needs a larger amount of thermal heat to be excited to the next excited state.

The probability of the occupation of the higher energy state decreases at low temperatures. And this probability is enhanced by the existence of the magnetic field due to quantum confinement effects, [37]. At high temperature, and for all values of magnetic field, the behavior of a specific heat is nearly the same and it acts like 1D behavior of C_v . Also, electrons

have sufficient thermal energy and therefore excitations have a small dependence on DOS.

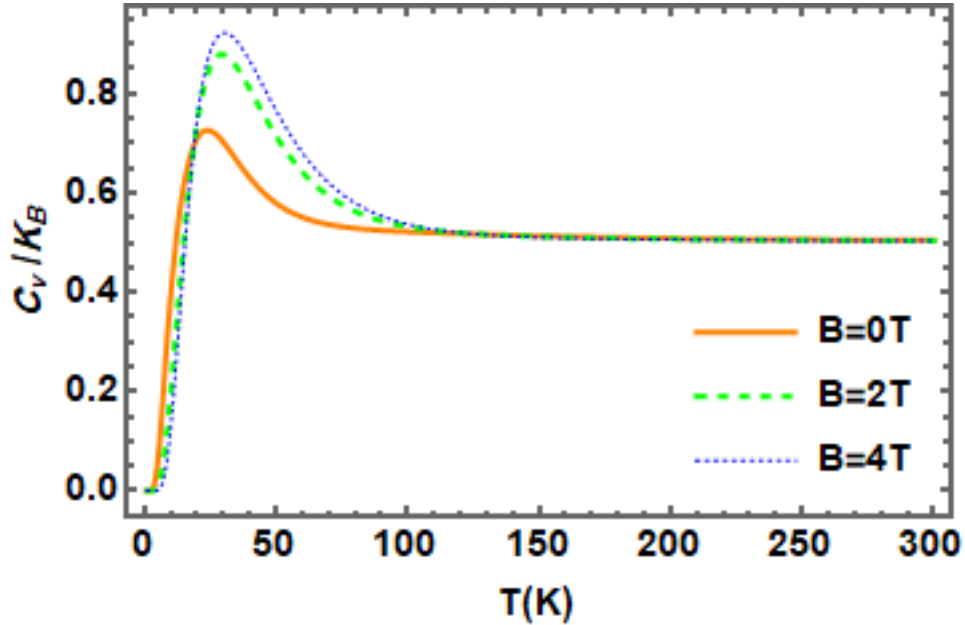


Fig 3.25 Variation of specific heat with temperature for different values of B ($B = 0\text{T}$ for solid line, $= 2\text{T}$ for dashed line, $= 4\text{T}$ for dotted line). At $\alpha_R=10\text{meV}\cdot\text{nm}$, and $\rho=5\text{nm}$.

The variation of specific heat of a quantum dot with RSOI parameter are shown in Fig. 3.26, for two different values of magnetic field $B = 5\text{ T}$, and 10T at $\rho=10\text{nm}$, and $T=10\text{K}$. From the figure, one can notice that the heat capacity decreases as RSOI parameter increases. Because spin-orbit interaction removes the degeneracy of the spin and more energy levels are exist in the unit range of energy. This cause reduction in the level spacing, so electron needs small amount of energy to be excited to the higher level. This behavior was shown in the previous figure 3.24 in which SOI lower the peak of heat capacity.

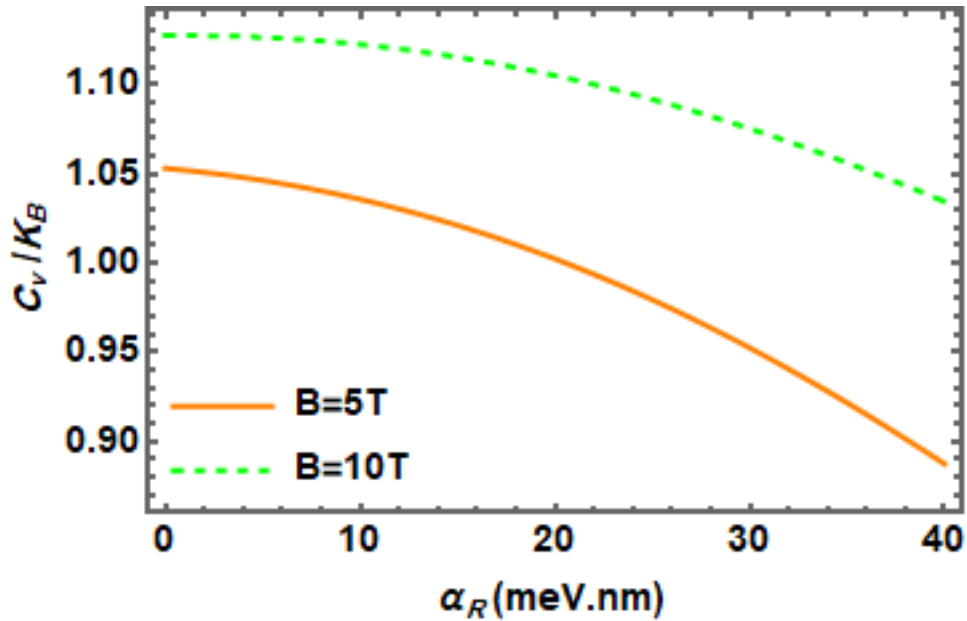


Fig .3.26: Heat capacity as a function of RSOI parameter for two different value of B (B=5T for solid line, =10T for dashed line). At T=10K, and $\rho=10\text{nm}$.

3.2.4 Entropy:

Entropy measures the randomness and disorder of the system. More randomness means more entropy.

The variation of entropy (S) with temperature are presented in Fig.3. 27 using eq. (2.27) for different values of α_R . as expected, as the temperature increases the entropy of a quantum dot increases also. This increase in entropy with temperature is due to enhancement of the thermal energy gained by the electron as a kinetic energy that makes more and more randomness in the system.

Whatever the value of B and T, the entropy is always higher in the presence of RSOI. This is because the RSOI lifts the degeneracy of the spin, yielding more energy states and thus more randomness, as shown in Fig.3.27.

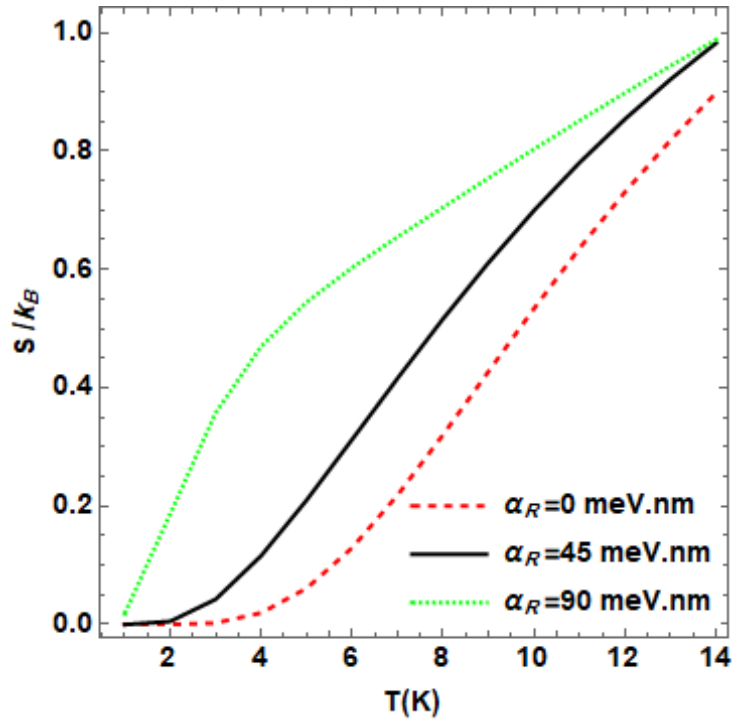


Fig.3.27: Entropy as a function of temperature at three different values of RSOI parameter ($\alpha_R=0$ mev.nm for dashed line, =45meV.nm for solid line, = 90 meV.nm for dotted line). At $B=5T$, and $\rho=10$ nm.

Variation of entropy with respect to the temperatures at different values of B is shown in Fig. 3.28. The entropy is enhanced as the temperature is increased for fixed value of B . However, comparing the behavior of entropy at lower temperatures with relatively higher temperatures yield to a big difference. For example, at relatively high temperature, entropy increases with temperature for all the values of B , and it becomes independent of the magnetic field at higher values of T . However, at low temperature, the behavior is very different and is clearly depends on the magnetic field, and the entropy is also found to be inversely proportional to the magnetic field. Because the increase in magnetic field restricts the particle motion to Landau-type levels, so disorder decreases and thus entropy, [38].

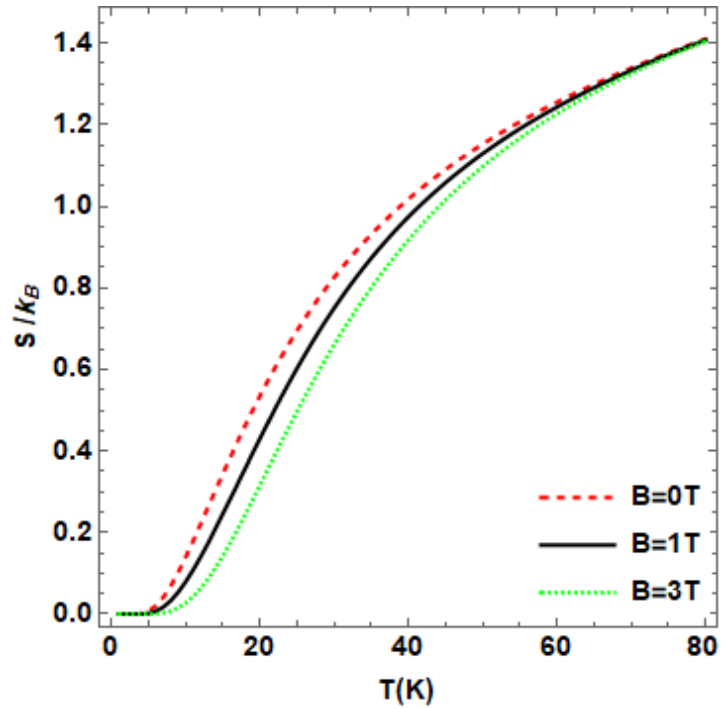


Fig. 3.28: Variation of entropy of InAs quantum dot with temperature at three different value of B (B=0T for dashed line, =1T for solid line, =3T for dotted line). At $\alpha_R=10$ meV.nm, and $\rho =5$ nm.

At high temperature, the entropy is found to be magnetic field independent due to the domination of thermal energy over magnetic energy [39].

To show the effect of changing radius of the cylindrical quantum dot on entropy, we have plotted in Fig3.29, the entropy as a function of T at different ρ - values. The figure shows that the entropy of a QD increases as the radius of the QD cylinder increases. And this behavior is due to increase in the range of motion, so the electron will be less confined, which leads to an increase in the disorder and thus entropy enhancement.

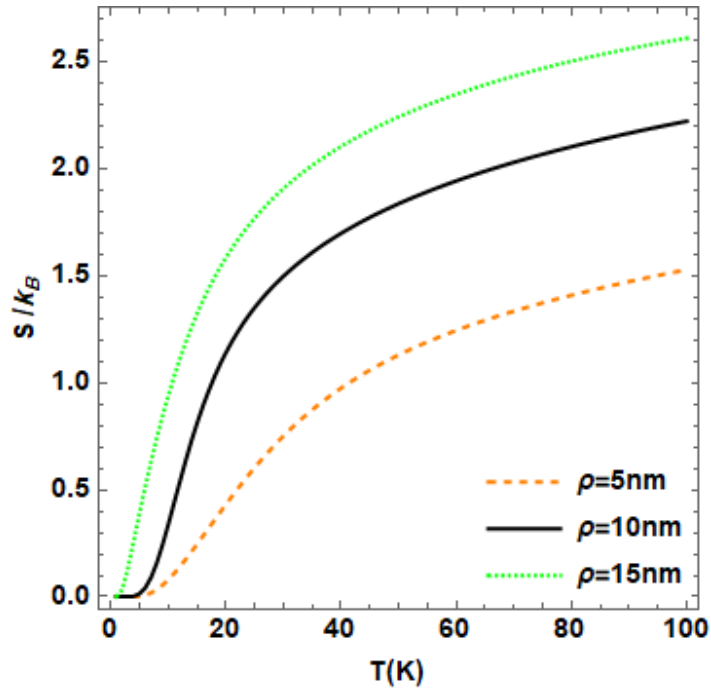


Fig.3.29: Variation of entropy of InAs quantum dot with temperature at three different value of ρ ($\rho=5\text{nm}$ for dashed line, $\rho=10\text{nm}$ for solid line, $\rho=15\text{nm}$ for dotted line). At $\alpha_R=10\text{meV}\cdot\text{nm}$, and $B=1\text{T}$.

The variation of entropy with RSOI parameter is shown in Fig 3.30. We notice that as α_R increases the entropy increases also, this is due to the effect of RSOI in lifting the degeneracy, so more energy levels exist and this lead to increase the electron's movement, so there will be more disorder resulting in an increase in the entropy .

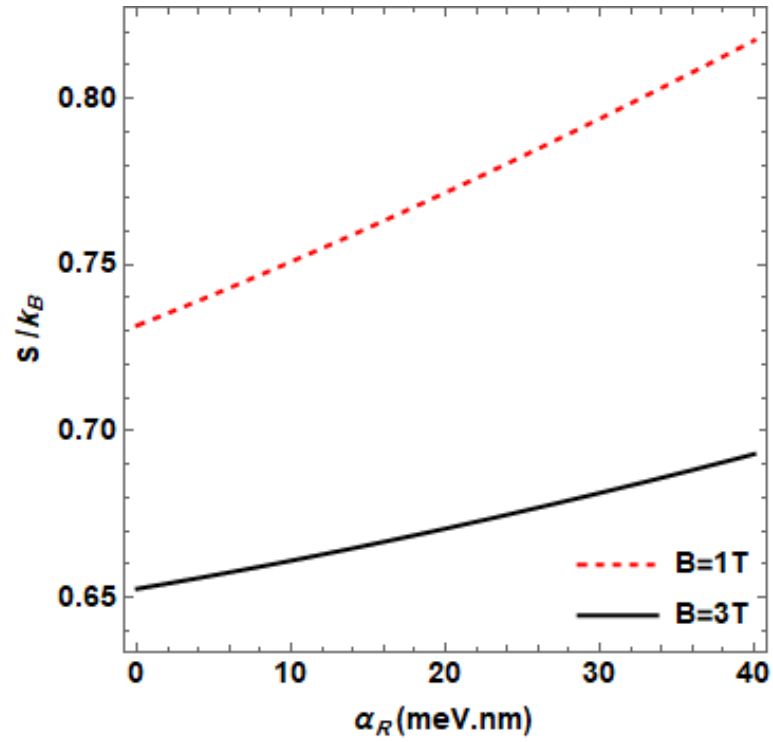


Fig.3.30: Variation of entropy of InAs quantum dot with RSOI parameter at two different value of B (B= 3T for solid line, =1T for dashed line). At T=30K and $\rho=5\text{nm}$.

Chapter Four

Conclusions

In this study, the eigenenergy spectra of the cylindrical QD's for GaAs and InAs materials in the presence of a magnetic field had been reproduced analytically, for zero and non-zero Rashba spin-orbit interaction term.

We have studied in the first part, the energy spectra for GaAs QD as a function of: pseudo potential strength (U_0), frequency of confinement potential (ω_0), cylindrical height (L), and magnetic field strength (B) for zero Rashba case. The energy spectra shows energy level crossings.

We have studied in the second part the energy spectra, for InAs QD, as a function of: Radius (ρ), Strength of magnetic field (B), and Rashba parameter (α_R). The energy spectra show a transition in the angular momentum of the electron energy states.

We have computed the average statistical energy with different physical parameters. The convergency of statistical energy is tested against the variation of the number of basis to ensure accurate numerical results. Our results show that the magnetic field strength (B), Rashba spin orbit parameter (α_R), frequency of confinement potential (ω_0) and the temperature (T) have a great significant effects on the average statistical energy.

In addition, we investigate theoretically the effects of magnetic field, Rashba parameter-strength and temperature on the variation of the magnetic

properties like magnetization and susceptibility of the GaAs –and InAs QD's. The variation of the magnetization and susceptibility with Rashba parameter is explicitly shown. All the curves of physical quantities for various temperature: $\langle E \rangle$, M , and χ , show an oscillating behavior against B for various temperatures. This behavior is attributed to the energy level crossings in the QD spectra. The susceptibility shows a magnetic phase changes from diamagnetic to paramagnetic type in a QD made from In-nanomaterial.

Finally, we present the behavior of the thermal properties of the studied QD's and investigate the effect of magnetic field strength and Rashba spin orbit interaction on thermal quantities like: heat capacity and entropy. The heat capacity shows a peak structure known as Schottky effect.

The present computed results are in agreement with the corresponding reported ones in literature.

References

- [1] Jeevanandam, J., Barhoum, A., Chan, Y. S., Dufresne, A., & Danquah, M. K. *Review on nanoparticles and nanostructured materials: history, sources, toxicity and regulations*. *Beilstein journal of nanotechnology*, 9(1), 1050-1074. (2018).
- [2] N.H. Abd Ellah, S.A. Abouelmagd. **Surface functionalization of polymeric nanoparticles for tumor drug delivery: approaches and challenges** *Expert Opin. Drug Deliv.* 1–14. (2016).
- [3] Henini, M. (Ed.). **Handbook of self-assembled semiconductor nanostructures for novel devices in photonics and electronics**. Elsevier. (2011).
- [4] G Rezaei and S Shojaeian Kish. *Effects of external electric and magnetic fields, hydrostatic pressure and temperature on the binding energy of a hydrogenic impurity confined in a two-dimensional quantum dot*. *Physica E: Low-dimensional Systems and Nanostructures*. 45:56–60. (2012).
- [5] Kailasa, S. K., Cheng, K. H., & Wu, H. F. *Semiconductor nanomaterials-based fluorescence spectroscopic and matrix-assisted laser desorption/ionization (MALDI) mass spectrometric approaches to proteome analysis*. *Materials*, 6(12), 5763-5795. (2013).
- [6] Shea-Rohwer, L. E., Martin, J. E., Cai, X., & Kelley, D. F. *Red-emitting quantum dots for solid-state lighting*. *ECS Journal of Solid State Science and Technology*, 2(2), R3112. (2012).

- [7] Pisanic Ii, T. R., Zhang, Y., & Wang, T. H. *Quantum dots in diagnostics and detection: principles and paradigms*. *Analyst*, 139(12), 2968-2981, (2014).
- [8] Zeng, Z., Garoufalis, C. S., & Baskoutas, S. *Combination effects of tilted electric and magnetic fields on donor binding energy in a GaAs/AlGaAs cylindrical quantum dot*. *Journal of Physics D: Applied Physics*, 45(23), 235102, (2012).
- [9] Ciftja, O. *Understanding electronic systems in semiconductor quantum dots*. *Physica Scripta*, 88(5), 058302. (2013).
- [10] <https://web.stanford.edu/group/MarcusLab/research.html>
- [11] Erdem, T., & Demir, H. V. *Color science of nanocrystal quantum dots for lighting and displays* *Nanophotonics*, 2(1), 57-81. (2013).
- [12] Frecker, T., Bailey, D., Arzeta-Ferrer, X., McBride, J., & Rosenthal, S. J. *Quantum dots and their application in lighting, displays, and biology*. *ECS Journal of Solid State Science and Technology*, 5(1), R3019- R3031. (2016).
- [13] Heidari Semiromi, E. *Spin resolved conductance in semiconductor mesoscopic rings: not spin gate response*. *Journal of Applied Physics*, 111(12), 124502. (2012).
- [14] Sarma, S. D. *Spintronics: A new class of device based on electron spin, rather than on charge, may yield the next generation of microelectronics*. *American Scientist*, 89(6), 516-523, (2001).

- [15] SAITO, Yoshiaki, et al. *Spin-based MOSFET and its applications*. **Journal of the Electrochemical Society**, 158.10: H1068-H1076. (2011).
- [16] Ikhdair, S. M., & Hamzavi, M. *A quantum pseudodot system with two-dimensional pseudo harmonic oscillator in external magnetic and Aharonov-Bohm fields*. **Physica B: Condensed Matter**, 407(21), 4198-4207. (2012).
- [17] Jahromi, A. S., & Rezaei, G. *Electromagnetically induced transparency in a two-dimensional quantum pseudo-dot system: Effects of geometrical size and external magnetic field*. **Physica B: Condensed Matter**, 456, 103-107, (2015).
- [18] Khosravi, M., Vaseghi, B., Abbasi, K., & Rezaei, G. *Magnetic Susceptibility of Cylindrical Quantum Dot with Aharonov-Bohm Flux: Simultaneous Effects of Pressure, Temperature, and Magnetic Field*. **Journal of Superconductivity and Novel Magnetism**, 1-8. (2019).
- [19] Li, Y., Voskoboynikov, O., Lee, C. P., Sze, S. M., & Tretyak, O. *Electron energy state dependence on the shape and size of semiconductor quantum dots*. **Journal of Applied Physics**, 90(12), 6416-6420, (2001).
- [20] Bogachek, E. N., Scherbakov, A. G., & Landman, U. *Temperature scales of magnetization oscillations in an asymmetric quantum dot*. **Physical Review B**, 63(11), 115323. (2001).

- [21] Gumber, S., Kumar, M., Gambhir, M., Mohan, M., & Jha, P. K. *Thermal and magnetic properties of cylindrical quantum dot with asymmetric confinement. Canadian Journal of Physics*, 93(11), 1264-1268. (2015).
- [22] Shaer, A., ELSAID, M., & Elhasan, M. *The magnetic properties of a quantum dot in a magnetic field .Turkish Journal of Physics*, 40(3), 209-218. , (2016).
- [23] Shaer, A., Elsaid, M. K., & Elhasan, M. *Magnetization of GaAs parabolic quantum dot by variation method. J. Phys. Sci. Appl*, 6(2), 39-46. (2016).
- [24] Kumar, D. S., Mukhopadhyay, S., & Chatterjee, A. *Magnetization and susceptibility of a parabolic InAs quantum dot with electron–electron and spin–orbit interactions in the presence of a magnetic field at finite temperature. Journal of Magnetism and Magnetic Materials*, 418, 169-174. (2016).
- [25] Alia, A. A., Elsaid, M. K., & Shaer, A. *Magnetic properties of GaAs parabolic quantum dot in the presence of donor impurity under the influence of external tilted electric and magnetic fields. Journal of Taibah University for Science*, 13(1), 687-695. (2019).
- [26] Elsaid, M. K., Alia, A. A., & Shaer, A. *Rashba spin-orbit interaction effects on thermal and magnetic properties of parabolic GaAs quantum dot in the presence of donor impurity under external electric*

- and magnetic fields. Chinese Journal of Physics*, (66), 335-348. (2020).
- [27] Elsaid, M. K., Shaer, A., Hjaz, E., & Yahya, M. H. *Impurity effects on the magnetization and magnetic susceptibility of an electron confined in a quantum ring under the presence of an external magnetic field. Chinese Journal of Physics*, 64, 9-17. (2020).
- [28] Hjaz, E., Elsaid, M. K., & Elhasan, M. *Magnetization of coupled double quantum dot in magnetic fields. Journal of Computational and Theoretical Nanoscience*,. 14(4), 1700-1705. (2017).
- [29] Elsaid M K, Hjaz E. *Magnetic Susceptibility of Coupled Double GaAs Quantum Dot in Magnetic Fields. Acta Phys Pol A*. 131(6). (2017).
- [30] Elsaid M, Hjaz E, Shaer A. *Energy states and exchange energy of coupled double quantum dot in a magnetic field. IntJ Nano Dimens*, 8(1): 1-8. (2017).
- [31] El-Said, Mohammad. "*The magnetoabsorption spectra of donors in a quantum well wire.*" *Semiconductor science and technology* 9, no. 10: 1787. (1994):
- [32] El-Said, M. O. H. A. M. M. A. D. "*The energy level ordering in two-electron quantum dot spectra.*" *Superlattices and microstructures* 23, no. 6: 1237-1243. (1998)
- [33] Azizi, V., & Vaseghi, B. *Electromagnetically induced transparency in a quantum pseudo-dot with spin-orbit interaction. Optical and Quantum Electronics*, 50(2), 93, (2018).

- [34] Gharaati, A. *Lande g-factor in semiconductor cylinder quantum dots under magnetic fields and spin-orbit interaction*. **Solid State Communications**, 258, 17-20, (2017).
- [35] Shaer, A., ELSAID, M., & Elhasan, M. *The magnetic properties of a quantum dot in a magnetic field*. **Turkish Journal of Physics**, 40(3), 209-218. (2016).
- [36] Gumber, S., Kumar, M., Jha, P. K., & Mohan, M. *Thermodynamic behaviour of Rashba quantum dot in the presence of magnetic field*. **Chinese Physics B**, 25(5), 056502, (2016).
- [37] Khordad, R., & Sedehi, H. R. *Thermodynamic properties of a double ring-shaped quantum dot at low and high temperatures*. **Journal of Low Temperature Physics**, 190(3), 200-212. (2018).
- [38] Boyacioglu, B., & Chatterjee, A. *Heat capacity and entropy of a GaAs quantum dot with Gaussian confinement*. **Journal of applied physics** 112(8), 083514, (2012).
- [39] Al Shorman, M. M., Nammas, F. S., Haddad, H., & Shukri, A. A. *Heat capacity and entropy of two electrons quantum dot in a magnetic field with parabolic interaction*. **Chinese journal of physics**, 56(3), 1057-1063. (2018)

Appendix A

The used notations in Eq .2.11 are as:

$$A_{11} = -k_z^2 \rho^2 - \beta_1 + \lambda_1 + \frac{2m^*}{\hbar^2} \rho^2 \varepsilon$$

$$A_{22} = -k_z^2 \rho^2 - \beta_2 + \lambda_2 + \frac{2m^*}{\hbar^2} \rho^2 \varepsilon$$

$$A_{12} = -i \frac{2m^*}{\hbar^2} \rho^2 k_z \alpha$$

$$A_{21} = i \frac{2m^*}{\hbar^2} \rho^2 k_z \alpha$$

Where ε is energy eigenvalues. The parameter β_1, β_2 and λ_1, λ_2 are defined as

$$\beta_1 = m \left[\frac{2m^* \alpha \rho}{\hbar^2} + m + \frac{eB}{\hbar} \rho^2 \right]$$

$$\lambda_1 = \frac{-6m^* \rho^2}{\hbar^2} - \frac{m^* g \mu_B B \rho^2}{\hbar^2} - \frac{e \alpha m^* \rho^3 B}{\hbar^3} - \frac{1}{4} \left(\frac{eB \rho^2}{\hbar} \right)^2$$

$$\beta_2 = (m+1) \left[-\frac{2m^* \alpha \rho}{\hbar^2} + (m+1) + \frac{eB}{\hbar} \rho^2 \right]$$

$$\lambda_2 = \frac{6m^* \rho^2}{\hbar^2} + \frac{m^* g \mu_B B \rho^2}{\hbar^2} + \frac{e \alpha m^* \rho^3 B}{\hbar^3} - \frac{1}{4} \left(\frac{eB \rho^2}{\hbar} \right)^2$$

Set the determinant of Eq. (2.11) equal to zero yield to:

$$\begin{vmatrix} A_{11} & A_{12} \\ A_{21} & A_{22} \end{vmatrix} = 0 \quad (A.1)$$

$$A_{11} A_{22} - A_{21} A_{12} = 0 \quad (A.2)$$

Where:

$$\begin{aligned}
A_{11}A_{22} &= k_z^4 \rho^4 + k_z^2 \rho^2 [\beta_1 + \beta_2 - \lambda_1 - \lambda_2] \\
&\quad + \frac{2 m^* \rho^2 \varepsilon}{\hbar^2} [\lambda_1 + \lambda_2 - \beta_1 - \beta_2] - \frac{4 k_z^2 m^* \rho^4 \varepsilon}{\hbar^2} \\
&\quad + \frac{4 m^* \rho^4 \varepsilon^2}{\hbar^4} \tag{A.3}
\end{aligned}$$

$$A_{21} A_{12} = \frac{-m^* \rho^4 k_z^2 \alpha^2}{\hbar^4} \tag{A.4}$$

So Eq.(A.2) become as squared equation :

$$\begin{aligned}
\frac{4 m^* \rho^4 \varepsilon^2}{\hbar^4} - \frac{2 m^* \rho^2}{\hbar^2} [2 k_z^2 \rho^2 - \lambda_1 - \lambda_2 + \beta_1 + \beta_2] \varepsilon + k_z^4 \rho^4 \\
+ k_z^2 \rho^2 [\beta_1 + \beta_2 - \lambda_1 - \lambda_2] + \frac{-m^* \rho^4 k_z^2 \alpha^2}{\hbar^4} \\
= 0 \tag{A.5}
\end{aligned}$$

which have a general solution :

$$\text{with, } \varepsilon = \frac{-b \pm \sqrt{b^2 - 4ac}}{2a} \tag{A.6}$$

Where:

$$\begin{aligned}
a &= \frac{4 m^* \rho^4}{\hbar^4} \\
b &= -\frac{2 m^* \rho^2}{\hbar^2} [2 k_z^2 \rho^2 - \lambda_1 - \lambda_2 + \beta_1 + \beta_2]
\end{aligned}$$

$$c = k_z^4 \rho^4 + k_z^2 \rho^2 [\beta_1 + \beta_2 - \lambda_1 - \lambda_2] + \frac{-m^* \rho^4 k_z^2 \alpha^2}{\hbar^4}$$

Substitute that parameter into Eq. (A.5) and make few simplification yield

to:

$$\begin{aligned}
\varepsilon &= \frac{2 m^* \rho^2}{\hbar^2} [2 k_z^2 \rho^2 - \lambda_1 - \lambda_2 + \beta_1 + \beta_2] \\
&\quad \pm \frac{1}{4} \sqrt{(4 k_z \alpha)^2 + \frac{\hbar^4}{m^{*2} \rho^4} (\lambda_1 - \lambda_2 + \beta_1 + \beta_2)} \tag{A.7}
\end{aligned}$$

جامعة النجاح الوطنية

كلية الدراسات العليا

تأثير المجال المغناطيسي وظاهرة رشبا على الخصائص
المغناطيسية والحرارية لإلكترون محصور في نقطة كمية
شبه موصلة أسطوانية الشكل

إعداد

هناء سمير عبد الفتاح رجب

إشراف

أ.د. محمد السعيد

قدمت هذه الأطروحة استكمالاً لمتطلبات الحصول على درجة الماجستير في الفيزياء بكلية

الدراسات العليا في جامعة النجاح الوطنية في نابلس، فلسطين

2021

ب
تأثير المجال المغناطيسي وظاهرة رشبا على الخصائص المغناطيسية والحرارية لإلكترون
محصور في نقطة كمية شبه موصلة أسطوانية الشكل

إعداد
هناء سمير عبد الفتاح رجب
إشراف
أ.د محمد السعيد

الملخص

قمنا بدراسة تأثير المجال المغناطيسي و ظاهرة رشبا على الخصائص المغناطيسية و الحرارية لنقطة كمية من مادتي GaAs و InAs عن طريق حساب مستويات الطاقة لهذه النقطة باستخدام طريقة حساب قطرية المصفوفة. تم استخدام مستويات الطاقة في حساب التمعنط للنقطة الكمية ودراسة تأثير كل من قوة المجال المغناطيسي ودرجة الحرارة وتردد القطع على كل من مستويات الطاقة و التمعنط و النفاذية المغناطيسية و الحرارة النوعية و معامل العشوائية لهذه النقطة. بالاضافة الى ذلك, تم دراسة تأثير (الرشبا المغزلي) على الخصائص المغناطيسية و الحرارية للنقطة الكمية، حيث أن لهذا العامل دور مهم في مجال الالكترونيات المعتمدة على غزل الالكترون "Spintronics" وكانت النتيجة ان وجود المجال المغناطي , درجة الحرارة, تردد الحصر, بالاضافة الى تأثير الرشبا يؤثر على الخصائص المغناطيسية و الحرارية للنقطة الكمية، حيث تتغير الطبيعة المغناطيسية للمادة بتغيير قيم هذه المتغيرات. كما أن الحرارة النوعية و معامل العشوائية للنقطة الكمية تتأثر بتغيير قيم هذه المتغيرات.

وكانت النتائج التي حصلنا عليها متوافقة بشكل جيد مع نتائج منشورة سابقا .